Compositional effects on the hydrogen cycling stability of multicomponent Ti-Mn based alloys

Nayebossadri, Shahrouz; Book, David

DOI:
10.1016/j.ijhydene.2019.02.138

Document Version
Peer reviewed version

Citation for published version (Harvard):
Nayebossadri, S & Book, D 2019, 'Compositional effects on the hydrogen cycling stability of multicomponent Ti-Mn based alloys', *International Journal of Hydrogen Energy*, vol. 44, no. 21, pp. 10722-10731. https://doi.org/10.1016/j.ijhydene.2019.02.138

Elsevier Editorial System(tm) for
International Journal of Hydrogen Energy
Manuscript Draft

Manuscript Number: HE-D-18-04640R1

Title: Compositional effects on the hydrogen cycling stability of multicomponent Ti-Mn based alloys

Article Type: Full Length Article

Section/Category: Hydrides / Hydrogen Storage

Keywords: Metal hydrides; Ti-Mn based alloys; C14 Laves phase; hydrogen cycling

Corresponding Author: Dr. Shahrouz Nayebossadri, PhD

Corresponding Author's Institution: University of Birmingham

First Author: Shahrouz Nayebossadri, PhD

Order of Authors: Shahrouz Nayebossadri, PhD; David Book

Abstract: Intermetallic alloys such as AB, AB2, and AB5 type have been studied due to their capability to reversibly store hydrogen. These alloys exhibit varying hydrogen storage properties depending on the crystal structure and composition. Compositional modification is commonly known as an effective method to modify the alloys thermodynamic and kinetics for various applications such as metal hydride batteries, metal hydrides hydrogen storage and compression. However, the effects of the compositional modification on the cyclic stability of these alloys are not usually well studied.
Here, the hydrogen cycling stabilities of Ti-Mn based alloys with C14 type structure are studied. Hyper-stoichiometry, stoichiometry and hypo-stoichiometry alloys were prepared accordingly: $Ti_{30.6}V_{16.4}Mn_{48.7}$ ($Zr_{0.7}Cr_{0.8}Fe_{2.8}$) (B/A=2.19), $Ti_{32.8}V_{15.1}Mn_{47.1}$ ($Zr_{0.9}Cr_{1.2}Fe_{2.9}$) (B/A=1.97) and $Ti_{34.5}V_{15.4}Mn_{44.7}$ ($Zr_{0.9}Cr_{1.3}Fe_{3.2}$) (B/A=1.87). Whilst the hyper-stoichiometry alloy showed almost a stable (about 9 % capacity reduction) hydrogen capacity after 1000 cycles of hydrogenation and dehydrogenation, the stoichiometry and hypo-stoichiometry alloys failed to hydrogenate after about 950 and 500 cycles respectively. A limited reduction in the calculated crystalline size of the alloys was observed before and after the hydrogen cycling, denoting that pulverisation plays a less significant role on the observed hydrogen capacity loss. In addition, a reduction in the B/A ratio from 2.19 to 1.82 (hyper to hypo-stoichiometry) encouraged the formation of more stable hydride and a higher level of heterogeneous lattice strain. Whilst a small loss of hydrogen capacity (9%) in the hyper-stoichiometry alloy was attributed to the trapped hydrogen, the complete loss of hydrogen capacity in the stoichiometry and hypo-stoichiometry alloys seemed to originate from the formation of stable hydride and the lattice distortion.

Compositional effects on the hydrogen cycling stability of multicomponent Ti-Mn based alloys

Shahrouz Nayebossadri and David Book
School of Metallurgy and Materials, University of Birmingham,
Edgbaston, Birmingham, B15 2TT, UK

Cover letter

The hydrogen cyclic stabilities of Ti-Mn based alloys with C14 type structure are studied as a function of the alloys composition. A Notable hydrogen capacity loss was observed as a result of B/A atomic ratio reduction. Only limited reduction in the crystalline size was observed, denoting pulverisation plays a less significant role on the observed hydrogen capacity loss. Hydrogen capacity loss appeared to be mainly occur through a dynamic mechanism caused by trapped atomic hydrogen and stable hydride phase formation. Our calculations shows that whilst hydrogen capacity loss as a result of trapped hydrogen can be recovered by appropriate heat treatment, hydride formation may induce levels of permanent hydrogen capacity loss due to the lattice distortion. This study helps to clarify the role of the alloys composition on the cyclic stability of the Ti-Mn based alloys critical for the development of durable hydrogen storage materials.

We appreciate that, if you could please consider this article for publication in the International Journal of Hydrogen Energy.

***Detailed Response to Reviewers**

Click here to download Detailed Response to Reviewers: Reply to the reviewrs comments.docx

Date: 12-23-2018
To: "Shahrouz Nayebossadri" s.nayebossadri@bham.ac.uk
From: Søren Juhl Andreasen eesserver@eesmail.elsevier.com
Reply To: Søren Juhl Andreasen sja@serenergy.com
Subject: Your Submission - HE-D-18-04640

Manuscript Number: HE-D-18-04640
Title: Hydrogen cycling stability of multicomponent Ti-Mn based alloys as a function of stoichiometry
Article Type: Full Length Article
International Journal of Hydrogen Energy

Reviewers' comments:

We appreciate your valuable comments and the recommendation. All changes are highlighted in the manuscript. Please review the revised manuscript and consider it for publication in the International Journal of Hydrogen Energy.

Reviewer #1: Manuscript Number: HE-D-18-04640
Title: Hydrogen cycling stability of multicomponent Ti-Mn based alloys as a function of stoichiometry

The current manuscript deals with the synthesis, characterisation and testing on the cyclic behaviour during hydrogenation/dehydrogenation of three samples based on the Ti-Mn family with some stoichiometric modifications. Although the manuscript presents some results and analysis, there are several issues that at the moment prevent it from acceptance for publication. I believe that a major revision is required before the manuscript will be considered for publication. My comments to the authors are listed as follows:

1) Title: The sentence function of stoichiometry is a bit of unclear and mostly refers to a mathematical relationship; maybe the authors should consider modifying this expression and/or the title to something more appropriate

The title is changed.

2) Abstract: The first sentence seems incomplete.

Modified.

3) Abstract: I would suggest the authors that in the abstract and for the whole manuscript not to use the hydrogen ab/desorption, but maybe something like: hydrogenation/dehydrogenation

Modified.

4) Abstract: The last 11 lines on the abstract provide an analysis that is not suitable to be included in that section; maybe the authors should consider to re-arrange into a more suitable format for the abstract

Modified.

5) Highlights; the first two are definitely not highlights - well known by the scientific community, I would suggest the authors to reconsider the highlights of their research and provide the actual highlights of their outcomes

Modified.

6) Introduction: There are references missing when referring to scientific facts, such as the end of line 2 (Page 2). Same as the end of line 5 (Page 2). The authors should consider adding some references to defend their statements.

References added.

7) In general, the manuscript seems to be prepared fast; several typos (line 16; Page 2) and although the manuscript comes from a UK-based University, there are some issues with the language as well; I would recommend that the authors should revisit the manuscript carefully and correct all the mistakes

We have revisited the manuscript and modified typos and the language.

8) Line 19; Page 2. The authors mention that 2wt% is acceptable; they should clarify for what type of application(s) is acceptable

Added.

9) Line 9; Page 3: The authors should make a comment whether the 10000 cycles is an appropriate number of cycles

Please note that in this section we are reviewing the works carried out by other researchers on the similar alloys. We cannot comment on the suitability of number of cycles used by other researchers and the details of the experimental work and the alloys properties are well discussed in that reference. We are just trying to attract the reader's attention to the reasons behind the hydrogen capacity loss.

10) Line 12; Page 3: Large reduction in the capacity; the authors should provide with a value to complete the picture

Corrected.

11) Line 16; Page 3: Heat treatment; the authors should provide more information

Added heat treatment condition according to the reference 19.

12) At the end of the Introduction; a final paragraph is missing that will clearly address the novelty of the present work comparing to previous published works and at the same time will introduce the reader to the upcoming scientific analysis

The last paragraph of the introduction summarises the outcome of the literature review and the possible reasons for the reported hydrogen capacity loss. Although some works have been done on the cyclic stability of the AB_2 alloys, there is no systematic study on the cyclic stability of these alloys with respect to their composition. This is stated in the last paragraph:

"In fact, most of the Laves phase AB_2 (particularly Ti-Mn based) alloys have been developed by compositional and structural modification for specific applications with limited attention to the cyclic stability of these alloys. This work studies the effect of alloy's stoichiometry on the cyclic stability of Ti-Mn based alloys under a similar experimental condition. The responsible mechanisms for hydrogen capacity loss and their relationship to the alloys composition is investigated."

13) Line 6; Page 6; The authors should clarify if the activation occurred once or in several cycles

Clarified.

14) The authors should clarify a bit more the measurements they did at the commercial Sieverts (Hidden) and the 'home-made' one

More details are added.

15) I believe that the word synthesis is more appropriate rather than fabrication

Corrected.

16) At the results part: The authors are immediately present the results in Fig. 1, without even introducing the materials 1, 2 and 3. A simple table with the nominal (expected) stoichiometries will do the job.

The actual composition of the alloys are given in the abstract and Table 1. We have replaced the text to inform the reader of the alloys composition given in Table 1.

17) Last line of Page 6; Should it be A(V) and B(Zr, Fe, Cr) instead of A(Zr) and B(V, Fe, Cr)?

In these alloys, the A-elements tend to be from the IVA group, such as Ti, Zr, Hf and/or the lanthanides (La, Ce Pr, etc). The B-elements can be a variety of transition or non-transition metals with a preference for V, Cr, Mn or Fe (Sandrock, 1999). Similar to the AB_5 family, a wide variety of substitutions are possible for both A and B elements which allows for fine tuning of the PCT properties.

18) Last line at Page 6 and first line at Page 7;…. Which their quantity is more or less similar in all the alloys..I think that a further explanation needed.

Corrected.

19) Line 4 Page 7: leading to the formation…. I thought that this was the initial target of the synthesis; to achieve this stoichiometries… this expression must be clarified.

Corrected.

20) Line 7; Page 7: The authors should explain why the Ti content in their samples is higher as compared to other studies

Please note that we wrote comparable, not compared.

21) Is the phase A3B3O expected to arise? Some extra comments might be helpful

It is. This is mainly related to the synthesis process and the handling/storing conditions. Comments are added.

22) Line 7; Page 8: The authors should give the values for the mid-plateau pressures

Values added to the Table 2.

23) Lines 12-19; Page 8: The work that the authors are referring has been submitted and not yet peer reviewed and accepted; thus, at the moment, I don't think that can be used as a valid scientific reference to defend the outcomes

Reference 38 is removed.

24) In general, chapter 3 is written without using any sub-chapters to make the reading easier and to separate the results; I would highly recommend that the authors should carefully split the chapter 3 in to sub-chapters; for example 3.1 SEM Micrographs, 3.2 XRD etc..

We have split section 3 into synthesised alloys and cycled alloys. Each section follows a logical order for demonstrating the experimental results and should be now easier for the readers to follow.

25) There is no chapter 4; from chapter 3 directly to chapter 5

Corrected.

26) Same comment as comment 24 for chapter 5; please separate in various sub-chapters

We think chapter 4 (Discussion) should be presented as one. Please note that unlike the result section, each paragraph on the discussion is required to support and clarify the following points and the current format best fits the purpose.

27) Line 18; Page 11; I believe that further explanation is necessary for the lack of stable phase

The lack of hydride phase can be seen in Figure 2 after the cycling and the possible reasons (high plateau pressure and less favourable thermodynamic) are well discussed within the article.

28) Figure 7; there is some overlapping at the y-axis (numbering)

Corrected.

29) Line 2; page 12; seems closer to 180degC rather than 150degC

Corrected.

30) Line 16; Page 12; I believe that the sentence: saturates around 650 cycles… is a bit risky here, as the authors didn't go over 1000 cycles, so the further cycling behavior is not known

We have modified the sentence.

31) Lines 17-19; Page 13; Did the authors investigate the situation on the surface or it is an assumption?

Hydride formation is well known to start from the surface of the particles and progress towards the centre. The kinetic rate limiting step is therefore hydrogen diffusion through the formed hydride phase. The low level of hydrogen desorbed from the alloys 2 and 3 suggests that stable hydrides may mainly formed on the surface of particles, hindering subsequent hy/dehydrogenations at the experimental condition used in this study.

Reviewer #2: Overall the reported work is interested and the manuscript is well written. Minor corrections should be made

For figures, instead of mentioning it as Alloy 1, 2 and 3, stating the actual composition of the metal hydride would be preferable. Doesn't make the reader going through pages to find the exact composition values.

Please note that this is to make the article easier to read and follow. The alloys used in this study have 6 components which makes it difficult to repeat throughout the manuscript. It will also be more difficult for

the readers to compare the alloys if they are given by their composition. So, for the sake of simplicity, we are mentioning alloys 1 to 3. Also, it will be easier in the final article format to check the compositions.

Page 10 heterogeneous instead of heterogeneous

Corrected.

When making comparison it is better to state in terms of values to make the reader show the significance of comparison. For example, page 13 shows that "dehydrogenation of alloy 3 starts at higher temperature", so higher temperature in relation both Alloy 1 and 2? And how high? Other examples on same page are "higher hydride phase abundance", " lowered as the B/A ratio decreased"

We have included values for clarification.

***Highlights (for review)**

- Hydrogen capacity loss is less likely to originate from the pulverisation in the studied alloys
- Hydrogen capacity loss occurs by hydrogen trapping and the stable hydride formation
- Stable hydride formation results in a progressive capacity loss and structural degradation
- A dynamic mechanism for hydrogen capacity loss is proposed

Compositional effects on the hydrogen cycling stability of multicomponent Ti-Mn based alloys

Shahrouz Nayebossadri and David Book
School of Metallurgy and Materials, University of Birmingham,
Edgbaston, Birmingham, B15 2TT, UK

Abstract

Intermetallic alloys such as AB, AB_2, and AB_5 type have been studied due to their capability to reversibly store hydrogen. These alloys exhibit varying hydrogen storage properties depending on the crystal structure and composition. Compositional modification is commonly known as an effective method to modify the alloys thermodynamic and kinetics for various applications such as metal hydride batteries, metal hydrides hydrogen storage and compression. However, the effects of the compositional modification on the cyclic stability of these alloys are not usually well studied.

Here, the hydrogen cycling stabilities of Ti-Mn based alloys with C14 type structure are studied. Hyper-stoichiometry, stoichiometry and hypo-stoichiometry alloys were prepared accordingly: $Ti_{30.6}V_{16.4}Mn_{48.7}$ ($Zr_{0.7}Cr_{0.8}Fe_{2.8}$) (B/A=2.19), $Ti_{32.8}V_{15.1}Mn_{47.1}$ ($Zr_{0.9}Cr_{1.2}Fe_{2.9}$) (B/A=1.97) and $Ti_{34.5}V_{15.4}Mn_{44.7}$ ($Zr_{0.9}Cr_{1.3}Fe_{3.2}$) (B/A=1.87). Whilst the hyper-stoichiometry alloy showed almost a stable (about 9 % capacity reduction) hydrogen capacity after 1000 cycles of hydrogenation and dehydrogenation, the stoichiometry and hypo-stoichiometry alloys failed to hydrogenate after about 950 and 500 cycles respectively. A limited reduction in the calculated crystalline size of the alloys was observed before and after the hydrogen cycling, denoting that pulverisation plays a less significant role on the observed hydrogen capacity loss. In addition, a reduction in the B/A ratio from 2.19 to 1.82 (hyper to hypo-stoichiometry) encouraged the formation of more stable hydride and a higher level of heterogeneous lattice strain. Whilst a small loss of hydrogen capacity (9%) in the hyper-stoichiometry alloy was attributed to the trapped hydrogen, the complete loss of hydrogen capacity in the stoichiometry and hypo-stoichiometry alloys seemed to originate from the formation of stable hydride and the lattice distortion.

Keywords: *Metal hydrides, Ti-Mn based alloys, C14 Laves phase, hydrogen cycling*

1. Introduction

The reversible reaction of some solid-state materials and hydrogen can offer a viable route to safely store, compress and transport hydrogen in a compact way [1], [2]. There are several metals and alloys capable to form hydrides at a range of pressures and temperatures [1]. Unlike ionic and covalent hydrides with a fixed composition, metal hydrides demonstrate high versatility in their composition, hence interesting materials for various applications [2], [3]. In particular, intermetallic compounds are promising materials for hydrogen storage due to their highly tunable properties. However, the stoichiometry of the intermetallic compound and therefore their crystal structure seems to dictate their hydrogen storage properties [2].

AB_2 intermetallic alloys based on the Laves phase crystal structures of cubic C15 (prototype $MgCu_2$, Pearson cF24 and space group *Fd*-3*m*) or hexagonal C14 (prototype $MgZn_2$, Pearson hP12, space group p63/*mmc*) have been studied for hydrogen storage [4]–[6]. Extended compositional homogeneity range can be offered by the Laves phase structure as a result of the vacancy formation, substitution of sub-stoichiometric atom positions by super-stoichiometric atoms in the structure and occupation of interstitial sites by super-stoichiometric atoms. [7], [8]. In addition, A and B elements can be easily replaced by additional alloying elements in most Laves phases [9], hence facilitating the modification of hydrogen storage properties of AB_2 intermetallic alloys.

Laves phase Ti-Mn based alloys are appealing hydrogen storage materials due to their acceptable hydrogen capacity at room temperature (~2wt%, suitable for stationary applications), fast hydrogenation and dehydrogenation kinetics, good cyclic stability, easy activation and a relatively low cost [10], [11]. However, the alloys composition and the type

of substitutional elements can have a substantial effect on the hydrogen storage characteristics of the alloy. For instance, it was noted that hydrogen capacity and the cyclic stability of the alloy can be improved by increasing the volume fraction of $TiMn_2$ phase via keeping the Ti content of the alloy at an optimum level [12], [13]. The compositional dependent hydrogen storage properties have also led to numerous efforts for tuning the thermodynamic and kinetics of the Ti-Mn based alloys for specific applications by partially substituting A and B atoms with transitional metals [10], [14]–[18]. Nevertheless, besides the thermodynamic and kinetics improvements, other factors such as cyclic stability and sensitivity to gas impurities play an important role in the effective development of these alloys.

The effect of the pressure induced hy/dehydrogenation cycling on the performance of the $TiMn_{1.5}$, $Ti_{0.8}Zr_{0.2}Mn_{1.2}Mo_{0.1}$ and $Ti_{0.9}Zr_{0.1}Mn_{1.4}Cr_{0.4}V_{0.2}$ alloys were investigated [19]. The hydrogen capacity of the binary and multicomponent alloys were reduced by 30 % and 20 % respectively, after about 10000 cycles. Although cycling imposed lattice distortion, no stable hydride phase or phase disproportionation could be identified. The hydrogen capacity reduction was rather related to the surface poisoning by impurity gases. In another study [20], hydrogen capacity of the $TiMn_2$ ($Ti_{40}Mn_{60}$ at. %) alloy almost halved (0.59 H/M to 0.3 H/M) after only 31 cycles. In this case, degradation in hydrogen capacity was attributed to the formation of stable Ti-H phase and retained hydrogen in interstitial sites accompanied by increasing lattice expansion and heterogeneous strain as a function of cycles. Yet, the hydrogen capacity in this alloy could be almost fully recovered by heating the alloy at 400 °C for 1 h under argon. Compositional and structural changes in the C14 Laves phase were also held responsible for the loss of hydrogen capacity in Ti-Mn based alloys during cycling [21]. Whilst $Ti_{40}Mn_{60}$ alloy retained almost its full hydrogen capacity after 30 cycles, a slight

change in the C14 Laves phase composition and therefore atomic site occupancy in the $Ti_{39}Mn_{61}$ (at. %) alloy could drastically decrease the cyclic stability.

The cyclic properties and effects of impurities in the gas stream on the hyper-stoichiometry $Ti_{0.98}Zr_{0.2}V_{0.43}Fe_{0.09}Cr_{0.05}Mn_{1.5}$ alloy were investigated [22] and only a limited degradation (less than 5 %) in the hydrogen capacity of the alloy was observed after 2000 cycles under high purity hydrogen (99.999%). However, the effects of gas impurities were distinct as N_2 and CH_4 only reduced the hydrogenation kinetic, whereas O_2, CO, CO_2 and H_2O reduced the hydrogen capacity and cyclic stability of the alloy. It was especially noted that if O_2 presents higher than 0.03 wt % in the alloys, it can be detrimental to the formation of homogeneous microstructure of the Laves phase. Furthermore, long-term cyclic stability of the same alloy was studied under hydrogen (99.999 %) and no degradation in hydrogen capacity of the alloy was reported after 42400 cycles [23]. Cyclic stability of the $Ti_{0.98}Zr_{0.2}V_{0.43}Fe_{0.09}Cr_{0.05}Mn_{1.5}$ alloy was also examined [24] after synthesising with low-cost and low purity FeV and Ti sponge and only a limited reduction in hydrogen capacity occurred after 1000 cycles, similar to the alloy made from the high purity elements. Nevertheless, the importance of microstructural homogeneity to maintain the cyclic stability of AB_2 alloys is well established [12], [25]–[27].

2. Hence, it seems that the cyclic stability of Ti-Mn based alloys is controlled by the inherent properties of the alloys as well as the external factors. For example, thermodynamic preference of most intermetallic hydrides to form a stable elemental hydride can lead to a phase disproportionation and therefore reduced cyclic stability [28]. In the meantime, the effect of experimental conditions such as hydrogen gas purity, temperature range, cycling repetition time, gas pressure and alloy's handling [29] are equally important on the cyclic lifetime of the alloys. Evaluation of the alloys cyclic lifetime may become challenging if the

above factors are not examined systematically. In fact, most of the Laves phase AB_2 (particularly Ti-Mn based) alloys have been developed by compositional and structural modification for specific applications with limited attention to the cyclic stability of these alloys. This work studies the effect of alloys stoichiometry on the cyclic stability of Ti-Mn based alloys under a similar experimental condition. The responsible mechanisms for hydrogen capacity loss and their relationship to the compostion of the alloys are investigated.

2. Experimental details

Three (hypo-stoichiometry, stoichiometry and hyper-stoichiometry) alloys were synthesised from elements. Elemental Ti (sponge, 99.95%), V (pieces, 99.7%), Mn (pieces, 99.9%), Zr (sponge 99.5%), Cr (pieces, 99.995%), Fe (pieces, 99.99%) and Ni (powder, 99 %) were purchased from Alfa Aesar. Alloys were pressed into pellets using an ATLAS automatic uniaxial press to produce a 2 g charge before synthesising by arc melting on a water-cooled copper crucible in an argon atmosphere. Remnant oxygen in the arc melting chamber was removed by melting a sacrificial oxygen getter before melting the alloys. The arc melting current was kept at 50 A to minimise the risk of losing elements during the arc strike. Each alloy was rotated and melted at least three times to ensure the homogeneity. No heat treatment was performed on the synthesised alloys and they were crushed to a particle size of less than 50 μm and kept inside an argon filled glove box.

Alloys microstructure and composition were analysed by a Joel 6060 Scanning Electron Microscope (SEM) equipped with an INCA 300 Energy Dispersive Spectrometer (EDS). Alloys were mounted in Bakelite and polished with silicon carbide papers before final polishing with OPA 1/4 micron suspension. Samples were cleaned using Acetone in a fume cupboard and dried with an electric hot air gun to avoid oxidation and surface pitting.

Room temperature X-Ray Diffraction (XRD) measurements were performed using a Bruker D8–Advanced diffractometer with monochromatic CuKα radiation (λ = 1.54056 Å). The XRD data was refined via a pseudo–Rietveld method with TOPAS Academic software [30] using published crystallographic information files (.cif) obtained from the Inorganic Crystal Systems Database [31].

Alloys were activated in-situ before Pressure Compositional Isotherm (PCI) measurement by heating the alloy to 300 °C and then admitting 100 bar H_2. Alloys were kept at this pressure for 4 h whilst cooling down to room temperature and vacuumed to approximately 10^{-6} mbar at the end of the sequence. The activation process was repeated at least three times for each sample to ensure a full activation. A volumetric Sieverts-type system (Hiden Isochema HTPS-2) was used for PCI measurements under high purity hydrogen (Air Products; BIP-Plus Hydrogen 99.99996 %). Before measurements, the sample volume was determined by helium pycnometry. PCI Measurements were performed between 0 and 100 bar H_2 at room temperature. Measurements were performed with a minimum holding time of 20 minutes to ensure no kinetic limitation for hy/dehydrogenation.

Room temperature cyclic hydrogenation and dehydrogenation measurements were performed on the activated alloys between 0 and 70 bar H_2 pressure (Air Products; BIP-Plus Hydrogen 99.99996 %) with a keeping time of 10 min at each pressure using another volumetric Sieverts-type system built by the Hydrogen Materials Group at the University of Birmingham. Sample temperature was monitored with a K-type thermocouple, directly in contact with the sample. Pressure transmitters (Maximum pressure of 200 bar) with an accuracy of ±0.25% were used to monitor changes in the hydrogen pressure during hydrogen cycling. The cycled alloys were examined by XRD, Differential Scanning Calorimetry (Netzsch DSC 204 HP) and Thermal Gravimetric Analysis (Netzsch TG 209) coupled with a

Hidden Analytical HAL IV Mass Spectrometry (MS). Approximately 30 mg of each alloy was loaded into TG/DSC and a heating rate of 2 °C/min and an Ar flow of 100 mL/min was applied.

3. Results

3.1 Synthesised alloys

Elemental composition of the alloys was analysed by EDS and the results are given in Table 1. In addition, SEM micrographs of the alloys after synthesise are shown in Fig. 1. All the alloys can be characterised by a dominant matrix phase which is accompanied by minor grey and dark phases. Formation of the minority phases with different morphology in Ti-Mn based alloys have been reported [14], [15], [17], [21] which seems to be controlled by the Ti and Mn content of the alloys. EDS results in Table 1 also indicate that all the alloys contain a small amount of other substitutional elements for A (Zr) and B (V, Fe, Cr) sites, which their quantities do not significantly vary in the matrix phase of the alloys. However, the compositional analysis of the matrix phase shows a trend that is a reduction in Mn content and an increase in the Ti content of the alloys. As a result, a distinct B/A atomic ratio for each alloy can be seen in Table 1, forming hyper-stoichiometry (Alloy 1), stoichiometry (Alloy 2) and hypo-stoichiometry (Alloy 3) alloys. The elemental composition of the minor grey and dark phases are also included in Table 1, revealing a higher Ti content at these regions, which is comparable to the previous studies [10], [14], [21]. Elemental composition of the grey phase shows a very close Ti and Mn content for all the alloys, hence denoting the possible formation of TiMn phase. The volume fraction of the TiMn phase may be increased by decreasing the Mn content of the alloy. However, the formation of TiMn phase is not desirable as the hydrogen absorbed in this phase can be hardly desorbed [21]. The Ti content of the dark phase also seems to be significantly higher than the matrix phase, which

can potentially lead to the formation of stable Ti-H phase during the cycling. The compositional variation in the grey and dark phases are also reflected by a significant reduction in their respecting B/A atomic ratio.

The XRD patterns for the Alloys 1, 2 and 3 after synthesise are given in Fig. 2a, 3a and 4a respectively. All the alloys contain $TiMn_2$ phase with a C14 Laves phase structure and no minority phases can be detected. The XRD patterns of the Alloy 1 and 2 also show the existence of η-carbide type oxide A_3B_3O phase (FCC structure) [32], [33], where A=Ti and Zr and B=Mn and V. Rietveld refinement results in Table 2 provides a phase abundance of FCC oxide phase as approximately 1 % and 7.7 % for the Alloy 1 and 2 respectively, whilst the Alloy 3 seems to be fully composed of C14 Laves phase. The oxide phase formation is mainly related to the alloys synthesis and handling processes, hence all the alloys were stored under an inert atmosphere to avoid a possible increase in the oxide content. In addition, the substitutional elements observed by EDS analysis in Table 1, could not encourage the formation of any new phases in the alloys. The capability of substitutional elements to occupy the atomic crystallographic positions of typical primary phase constituents creates a large structural homogeneity region in the C14 Laves phase [9], [34], [35]. This offers the opportunity to improve the hydrogen storage characteristics of the C14 Laves phase by partial elemental substitution [6], [36], [37].

Room temperature hy/dehydrogenation PCI curves of the alloys are shown in Fig. 5. All the alloys show a single plateau for hy/dehydrogenation with a very similar maximum hydrogen capacity of approximately 1.7 %. The (mid) plateau pressures are highest for the Alloy 1 and lowest for the Alloy 3 (Table 2). The relationship is reversed in terms of C14 Laves phase unit cell volume of the alloys after the synthesis (Table 2), with the Alloy 1 possessing the smallest and the Alloy 3 the largest. The significant effect of C14 Laves phase unit cell

volume on the thermodynamics of the AB_2 type alloys has been studied [38], [39] and it was revealed that there is a less favourable thermodynamic for hydride formation as the C14 Laves phase unit cell volume is reduced. In fact, thermodynamic properties of the Ti-Mn based alloys could be tuned for specific applications by altering the C14 Laves phase unit cell volumes through the modification of Ti and Mn content of the alloys [18], [9], [35], [40], [41]. Also, the level of hysteresis seems to decrease from the Alloy 1 to the Alloy 3, whilst plateau slope increases. Although compositional modification seems to be an effective method to reduce the plateau slope in Ti-Mn base alloys, the level of hysteresis seemed to be mainly dictated by the thermodynamics of the alloy.

3.2 Cycled alloys

A typical cyclic measurement and the cyclic stability of the alloys under hydrogen are shown in Fig 6a and b. All the alloys were cycled under hydrogen between 0 and 70 bar whilst monitoring changes in the thermal profile of the samples showing exo/endotherms for hy/dehydrogenation respectively (Fig.6a). In-situ hydrogen capacity measurements were performed at specific points by disrupting the cyclic measurements (Fig 6b). The hydrogen capacity of the Alloy 1 appears to be stable until 250 cycles, where it slowly starts to decrease (about 9 %) until 650 cycles and then becomes stable again up to over 1000 cycles. In contrast, Alloys 2 and 3 show a progressive reduction in their hydrogen capacity until the alloys fail to hydrogenate after 970 and 500 cycles respectively. Hydrogen capacity recovery was performed at the end of the cyclic measurements by heat treating the alloys under 1 bar hydrogen at 350 °C for 24 h. It seems that hydrogen capacity can be fully recovered for the Alloys 1 and 2, whereas the Alloy 3 only regains about 80 % of its original hydrogen capacity (Fig. 6b).

The XRD patterns of the cycled alloys are given in Fig. 2b, 3b and 4b. Alloy 1 preserves it's C14 Laves phase structure after the cycling (Fig. 2b), and the formation of any new phase/s cannot be observed. However, XRD patterns of the Alloys 2 and 3 signify the formation of stable $TiMn_2$ hydride phase along with their original C14 Laves phase (Fig 3b and 4b). The XRD patterns of the alloys after hydrogen capacity recovery (heat treated at 350 °C and 1 bar H_2) are given in Fig. 2c, 3c and 4c, indicating only the existence of C14 Laves phase. Structural refinement results in Table 2 provides a phase abundance of the hydrogen cycled and heat treated alloys. Whilst, Alloy 1 is entirely composed of C14 Laves phase, Alloys 2 and 3 show the formation of approximately 13.5 % and 72.7 % of stable $TiMn_2$ hydride phase respectively, along with their remaining C14 Laves phase. Nevertheless, the structures of the Alloys 2 and 3 can be fully reverted to the C14 Laves phase after the heat treatment (Fig. 3c and 4c).

The lattice parameters and the C14 Laves phase unit cell volume of the alloys after cycling and heat treatment are also listed in Table 2. The lattice parameters and therefore C14 Laves phase cell volume increase in all the alloys after hydrogen cycling. However, Alloy 1 shows the least volume expansion of 0.17 % compared to the much larger volume expansions of 2.32 % in the Alloy 2 and 3.65 % in the Alloy 3. It seems that the volume expansion of C14 Laves phase remains to some extent in the Alloys 2 (0.42 %) and 3 (0.5 %) after the heat treatment, despite their full dehydrogenation as showed by XRD patterns in Fig. 3c and 4c. Minimal changes in the C14 unit cell volume of the Alloy 1 denotes a higher structural stability and the least changes in hydrogenation characteristics of the Alloy1 during hydrogen cycling.

XRD pattern of the C14 Laves phase in all the alloys also shows peak broadening after the hydrogen cycling. In general, XRD peak broadening after the hydrogen cycling can be

attributed to a decrease in crytalline size and/or generation of heterogeneous strain [12], [21]. High density dislocation formation as a result of lattice parameters mismatch of the hydride phase and the alloy and retained hydrogen are proposed as the origin of heterogeneous strain during the cycling [20], [25], [27]. Crystalline size and the heterogeneous strain induced during the cycling can be estimated from Hall's method [20], [42]:

$$\frac{\beta \cos\theta}{\lambda} = 2\eta \frac{\sin\theta}{\lambda} + \frac{1}{\varepsilon} \quad (1)$$

Where β is the Full Width at Half Maximum Intensity (FWHMI), θ is the peak postion, λ is the wavelength of the x-ray (0.15405 nm), η is the hetrogeneous strain and ε is the crytalline size. Crystalline size and heterogeneous strain of the alloys were estimated from Eq. (1) and are listed in Table 2. The crystalline size for all the alloys decreases after the cycling and some limited regrowth in the crystalline size seems to occur after the heat treratment. Heterogeneous strain increases in all the alloys after the cycling but its magnitude is lowest for the Alloy 1 (given by stress ratio in Table 2) and highest for the Alloy 3. In addition, heat treatment seems to almost fully relief the heterogeneous strain in the Alloys 1 and 2, but the remained heterogeneous strain in the Alloy 3 is almost double the value of this alloy after the synthesis.

4. Discussion

The observed unique cycling behaviour for each of the studied alloys signifies the important role of the alloy composition and structure on the cyclic lifetime. Although a relatively stable cyclic performance was reported for AB_2 type hydrides [21]–[24], The alloy composition seems to critically impact the cyclic property of the alloy. Here, the inherent properties of the alloys appear to be influenced as a result of a subtle change in the composition of the alloy. Degradation in cyclic stability of the studied alloys could be

occurred via pulverisation and/or phase disproportionation. The estimated crystalline size in Table 2, indicated a limited and nearly similar reduction in the crystalline size for all the alloys. Hence, the observed difference in the cyclic stability of the alloys is less likely to originate from the pulverisation. On the other hand, phase disproportionation could be seen in the Alloys 2 and 3 leading to the formation of stable hydride phase. In fact, it has been suggested that microstructural inhomogeneity as a result of changes in the alloys stoichiometry could potentially lead to disproportionation through the formation of stable hydride phases [27].

Dehydrogenation of the studied alloys was also investigated by TG-MS in Fig. 7. Surprisingly, hydrogen is also desorbed from the Alloy 1 (Fig. 7a), despite the lack of stable hydride phase after the cycling in this alloy (Fig.2b). TG curve of the Alloy 1 in Fig. 7b shows that the amount of released hydrogen is almost 0.1 wt %, which is close to the observed capacity loss of about 0.15 wt % at the end of the cycling (Fig. 6b). Although the proportion of the stable hydride phase in the Alloy 3 was higher compared to the Alloy 2 after the hydrogen cycling (Table 2), the amount of released hydrogen from the Alloy 2 (~0.4 wt %) is approximately twice the amount of hydrogen released from the Alloy 3 (~ 0.2 wt %) in Fig. 7b. In addition, TG curves in Fig. 7b indicates that hydrogen is more loosely retained in the Alloys 1 and 2 as the dehydrogenation starts at around 180 °C compared to 300 °C for the Alloy 3.

The TG-MS data clearly indicate the effect of the retained hydrogen for capacity loss during the cycling. In fact, structural changes and deviation of Mn atomic position as a function of C14 Laves phase composition in Ti-Mn based alloys were observed [21] during hydrogen cycling. This could result in retained hydrogen inside the Laves phase which its scale gradually increased during the hydrogen cycling. The retained hydrogen was accompanied

by heterogeneous strain and lattice expansion and its attenuating effect on hydrogen capacity was reported [18], [11], [25]. Hence, it seems that retained hydrogen, which is accompanied by a small increase in the lattice constants and C14 Laves phase volume, is the primary reason for the observed loss of hydrogen capacity in the Alloy 1. Nevertheless, hyper-stoichiometry of the Alloy 1 and its smaller C14 Laves phase cell volume seems to infer a higher cyclic stability at the beginning of the hydrogen cycling. Gradual changes in the C14 Laves phase structure (as evident from its lattice parameters and the cell volume) may lead to an increasing level of retained hydrogen that becomes noticeable between 250 to 650 cycles. Despite, the hydrogen interaction with the studied alloys during the cycling appears to be changing according to the alloys stoichiometry. Formation of stable hydride phase was observed in both Alloys 2 and 3 with lower B/A ratio (1.97 and 1.82 respectively) compared to the Alloy 1 (2.19) after the hydrogen cycling. Extended compositional homogeneity range in C14 Laves phase implies considerable changes in certain atomic and interstitial site occupation may occur as a result of changes in the composition of the alloy. Compositional changes may encourage the formation of interstitial sites with different local chemical environments. For example, the introduction of Ti into the B sites can create a series of interstitial sites rich in Ti, showing different affinities to hydrogen [43]. It was shown that [44] the excess Ti atoms in $Ti_{1.2}Mn_{1.8}$ alloy occupy one of the Mn atomic positions, preferably *2a* sites, leading to the formation of the Ti_3Mn interstitial site with high hydrogen affinity. Increasing the Ti content in the multicomponent alloys were also noted to enhance the alloy-hydrogen interaction [13]. The hydrogenation plateau pressures of the studied alloys lowered as the B/A ratio decreased (Fig. 5 and Table 1), indicating a more favourable thermodynamic for hydride formation. This was reflected in the higher phase abundance of the formed stable hydrides in the Alloys 3 (72.7 %) compared to the Alloy 2

(13.5 %), in accordance with their Ti content. However, a higher amount of hydrogen desorbed from the Alloy 2 compared to the Alloy 3 after the hydrogen cycling (Fig. 7b) may also be attributed to the contribution of retained hydrogen in the lattice rather than just dehydrogenation of the stable hydride phase. This can be corroborated by the similar dehydrogenation onset temperature (~ 180 °C) of the Alloy 2 to the Alloy 1 with no sign of stable hydride formation after the hydrogen cycling. In contrast, dehydrogenation of the Alloy 3 starts at a higher temperature (~ 300 °C) which may be entirely attributed to the dehydrogenation of the stable hydride phase observed after the hydrogen cycling. It is worth mentioning that the level of the hydrogen released from the Alloy 2 and especially Alloy 3 with a higher hydride phase abundance is well below the observed maximum hydrogen capacity of the alloys (~ 1.7 wt %). This may suggest that the stable hydrides are predominantly formed on the surface of the alloys, which could kinetically inhibit hy/dehydrogenation of the alloys at the studied experimental conditions.

Also, it was shown in Fig. 6b that the hydrogen capacity could be only fully recovered in the Alloys 1 and 2 after the heat treatment. Although heat treatment completely reverts the structure of the Alloys 2 and 3 to C14 Laves phase (Table 2), the volume expansion of the Alloys 2 and 3 remains at 0.42 % and 0.5 % respectively. Furthermore, unlike the Alloy 2 which its volume expansion does not lead to an increased heterogeneous strain ratio, the volume expansion in the Alloy 3 is accompanied by a higher heterogeneous strain ratio compared to this alloy after the synthesis. This may be explained by the variation of *c/a* ratio of the C14 Laves phase as given in Table 2. The *c/a* ratio of the Alloy 2 after heat treatment is almost similar to the original value after the synthesis. In contrast, the *c/a* ratio of the Alloy 3 after the heat treatment is considerably smaller compared to its value after the synthesis, denoting a non-uniform hexagonal cell expansion along the *a* axis. It is known

that [45] C14 Laves phase can be permanently deformed as a result of variation in its lattice parameters when interacting with hydrogen. It may be suggested that the higher level of hydride formed in the Alloy 3 deformed the C14 laves phase structure (e.g. by escalated dislocation density). Hence, the observed structural changes in the Alloy 3 may be responsible for the lack of full hydrogen capacity recovery after the heat treatment.

Overall, the observed loss of capacity during hydrogen cycling in the studied alloys appears to be a dynamic process, dominated by the alloy stoichiometry. Nevertheless, the cyclic stability of the alloys, particularly those with low hydrogenation plateau pressure, may be extended by tuning the experimental condition.

5. Conclusions

The effects of small stoichiometric changes on the microstructure, hydrogenation characteristics and particularly cyclic stability of the Ti-Mn based multicomponent alloys were investigated. The microstructure of hyper-stoichiometry (Alloy 1), stoichiometry (Alloy 2) and hypo-stoichiometry alloys featured a main C14 Laves phase accompanied by small secondary phases with considerably higher Ti contents. The hydrogenation characteristics of the alloys changed with respects to the alloys stoichiometry. Lowering B/A ratio reduced the hydrogenation plateau pressure. Cyclic stabilities of the alloys under high purity hydrogen were studied and hyper-stoichiometric alloy showed only about 9 % reduction in its hydrogen storage capacity after 1000 cycles as opposed to the full hydrogen capacity loss after about 950 cycles in the stoichiometry and about 500 cycles in the hypo-stoichiometry alloys. The loss of hydrogen capacity seemed to be caused by the retained hydrogen in C14 Laves phase lattice and/or the formation of stable hydride phase. However, this is a dynamic mechanism which suggested to be mainly determined by the composition of the alloy and to a lower extent by the experimental conditions, especially for the alloys with low

hydrogenation plateau pressures. Nevertheless, hydride formation during the cycling may cause levels of irreversible hydrogen capacity loss by gradually degrading the C14 Laves phase structure.

6. Acknowledgments

Support from the EPSRC Engineering Safe and Efficient Hydride-based Technologies (EP/K021117/1) and STFC Early Career Award (ST/N002385/1) is gratefully acknowledged. Authors would like to thank Professor David Grant, Professor Gavin Walker and Dr. Alastair Stuart for their support and guidance.

7. References

[1] D. F. Shriver and P. W. Atkins, *Inorganic Chemistry*, 3rd ed. London W. H. Freeman & Co, 1999.

[2] G. Sandrock, "A panoramic overview of hydrogen storage alloys from a gas reaction point of view," *J. Alloys Compd.*, vol. 293–295, pp. 877–888, Dec. 1999.

[3] N. A. A. Rusman and M. Dahari, "A review on the current progress of metal hydrides material for solid-state hydrogen storage applications," *Int. J. Hydrogen Energy*, vol. 41, no. 28, pp. 12108–12126, 2016.

[4] K. Young, T. Ouchi, J. Yang, and M. A. Fetcenko, "Studies of off-stoichiometric AB2 metal hydride alloy: Part 1. Structural characteristics," *Int. J. Hydrogen Energy*, vol. 36, no. 17, pp. 11137–11145, 2011.

[5] K. Young, J. Nei, B. Huang, and M. A. Fetcenko, "Studies of off-stoichiometric AB2 metal hydride alloy: Part 2. Hydrogen storage and electrochemical properties," *Int. J. Hydrogen Energy*, vol. 36, no. 17, pp. 11146–11154, 2011.

[6] K. Manickam, D. M. Grant, and G. S. Walker, "Optimization of AB2 type alloy composition with superior hydrogen storage properties for stationary applications," *Int. J. Hydrogen Energy*, vol. 40, no. 46, pp. 16288–16296, 2015.

[7] N. A. Kelly and R. Girdwood, "Evaluation of a thermally-driven metal-hydride-based hydrogen compressor," *Int. J. Hydrogen Energy*, vol. 37, no. 14, pp. 10898–10916, Jul. 2012.

[8] P. Muthukumar, M. Prakashmaiya, and S. Srinivasamurthy, "Experiments on a metal hydride based hydrogen compressor," *Int. J. Hydrogen Energy*, vol. 30, no. 8, pp. 879–892, Jul. 2005.

[9] S. V. Mitrokhin, "Regularities of hydrogen interaction with multicomponent Ti(Zr)–Mn–V Laves phase alloys," *J. Alloys Compd.*, vol. 404–406, pp. 384–387, Dec. 2005.

[10] M. Shibuya, J. Nakamura, and E. Akiba, “Hydrogenation properties and microstructure of Ti-Mn-based alloys for hybrid hydrogen storage vessel,” *J. Alloys Compd.*, vol. 466, no. 1–2, pp. 558–562, 2008.

[11] B.-H. Liu, D.-M. Kim, K.-Y. Lee, and J.-Y. Lee, “Hydrogen storage properties of TiMn2-based alloys,” *J. Alloys Compd.*, vol. 240, no. 1–2, pp. 214–218, 1996.

[12] S. Semboshi, N. Masahashi, and S. Hanada, “Effect of composition on hydrogen absorbing properties in binary TiMn2based alloys,” *J. Alloys Compd.*, vol. 352, no. 1–2, pp. 210–217, 2003.

[13] T. Gamo and Y. Moriwaki, “Formation and properties of titanium-manganese alloy hydrides,” *Int. J. Hydrogen Energy*, vol. 1, no. 1, pp. 39–47, 1985.

[14] M. Au, F. Pourarian, S. G. Sankar, W. E. Wallace, and L. Zhang, “TiMn2-based alloys as high hydrogen storage materials,” *Mater. Sci. Eng. B*, vol. 33, pp. 53–57, 1995.

[15] X. Yu, B. Xia, Z. Wu, and N. Xu, “Phase structure and hydrogen sorption performance of Ti-Mn-based alloys,” *Mater. Sci. Eng. A*, vol. 373, no. 1–2, pp. 303–308, 2004.

[16] M. . Hagström, J. . Vanhanen, and P. . Lund, “AB2 metal hydrides for high-pressure and narrow temperature interval applications,” *J. Alloys Compd.*, vol. 269, no. 1–2, pp. 288–293, 1998.

[17] L. Pickering, D. Reed, A. I. Bevan, and D. Book, “Ti-V-Mn based metal hydrides for hydrogen compression applications,” *J. Alloys Compd.*, vol. 645, no. S1, pp. S400–S403, 2015.

[18] R. R. Chen *et al.*, “Effects of Ti/Mn ratio on microstructure and hydrogen storage properties of Ti-V-Mn alloys,” *J. Alloys Compd.*, vol. 748, pp. 171–178, 2018.

[19] T. Gamo, Y. Moriwaki, N. Yanagihara, and T. Iwaki, “Life properties of TiMn alloy hydrides and their hydrogen purification effect,” *J. Less-Common Met.*, vol. 89, no. 2, pp. 495–504, 1983.

[20] S. Semboshi, N. Masahashi, and S. Hanada, “Degradation of hydrogen absobing capacity in cyclically hydrogenated TiMn2,” *Acta Mater.*, vol. 49, no. 5, pp. 927–935, 2001.

[21] S. Semboshi, M. Sakurai, N. Masahashi, T. J. Konno, and S. Hanada, “Effect of structural changes on degradation of hydrogen absorbing capacity in cyclically hydrogenated TiMn2based alloys,” *J. Alloys Compd.*, vol. 376, no. 1–2, pp. 232–240, 2004.

[22] D. Bernauer, O. Topler, J. Noresus, D. Hempelmann, R. Richter, “F U N D A M E N T A L S A N D PROPERTIES OF SOME Ti/Mn BASED LAVES PHASE HYDRIDES 0 .,” *Int. J. Hydrogen Energy*, vol. 14, no. 3, pp. 187–200, 1989.

[23] G. Friedlmeier, A. Manthey, M. Wanner, and M. Groll, “Cyclic stability of various application-relevant metal hydrides,” *J. Alloys Compd.*, vol. 231, no. 1–2, pp. 880–887, 1995.

[24] U. Ulmer, M. Dieterich, A. Pohl, R. Dittmeyer, M. Linder, and M. Fichtner, “Study of the structural, thermodynamic and cyclic effects of vanadium and titanium substitution

in laves-phase AB2hydrogen storage alloys," *Int. J. Hydrogen Energy*, vol. 42, no. 31, pp. 20103–20110, 2017.

[25] V. Iosub, J. M. Joubert, M. Latroche, R. Cerný, and A. Percheron-Guégan, "Hydrogen cycling induced diffraction peak broadening in C14 and C15 Laves phases," *J. Solid State Chem.*, vol. 178, no. 6, pp. 1799–1806, 2005.

[26] Y. Zhu, H. Pan, M. Gao, Y. Liu, and Q. Wang, "A study on improving the cycling stability of (Ti0.8Zr0.2)(V0.533Mn0.107Cr0.16Ni0.2)4 hydrogen storage electrode alloy by means of annealing treatment: I: Effects on the structures," *J. Alloys Compd.*, vol. 347, pp. 279–284, 2002.

[27] S. Selvaraj *et al.*, "Study of cyclic performance of V-Ti-Cr alloys employed for hydrogen compressor," *Int. J. Hydrogen Energy*, pp. 1–9, 2018.

[28] G. D. Sandrock and P. D. Goodell, "Cyclic life of metal hydrides with impure hydrogen: Overview and engineering considerations," *J. Less-Common Met.*, vol. 104, no. 1, pp. 159–173, 1984.

[29] R. C. Bowman, C. H. Luo, C. C. Ahn, C. K. Witham, and B. Fultz, "The effect of tin on the degradation of LaNi5-ySny metal hydrides during thermal cycling," *J. Alloys Compd.*, vol. 217, no. 2, pp. 185–192, 1995.

[30] A. Coelho, "Topas-Academic, Version 4.1, Coelho Software, Brisbane, Australia," 2007.

[31] D. A. Fletcher, R. F. McMeeking, and D. Parkin, "The United Kingdom Chemical Database Service," *J. Chem. Inf. Model.*, vol. 36, no. 4, pp. 746–749, 1996.

[32] J. Huot, E. Akiba, and Y. Ishido, "Crystal structure of multiphase alloys (Zr, Ti)(Mn, V) 2," *J. Alloys Compd.*, vol. 231, pp. 85–89, 1995.

[33] M. Shibuya, J. Nakamura, H. Enoki, and E. Akiba, "High-pressure hydrogenation properties of Ti–V–Mn alloy for hybrid hydrogen storage vessel," *J. Alloys Compd.*, vol. 475, no. 1–2, pp. 543–545, May 2009.

[34] S. . Mitrokhin, T. . Bezuglaya, and V. . Verbetsky, "Structure and hydrogen sorption properties of (Ti,Zr)–Mn–V alloys," *J. Alloys Compd.*, vol. 330–332, pp. 146–151, 2002.

[35] S. V Mitrokhin, T. N. Smirnova, V. A. Somenkov, V. P. Glazkov, and V. N. Verbetsky, "Structure of (Ti,Zr)-Mn-V nonstoichiometric Lavas phases and (Ti0.9Zr0.1)(Mn0.75V0.15Ti0.1D2.8 deuteride," *J. Alloys Compd.*, vol. 357, pp. 80–83, 2003.

[36] J. L. Bobet, B. Chevalier, and B. Darriet, "Crystallographic and hydrogen sorption properties of TiMn2 based alloys," *Intermetallics*, vol. 8, no. 4, pp. 359–363, 2000.

[37] J. D. Livingston, "Laves-phase superalloys?," *Phys. Status Solidi*, vol. 131, no. 2, pp. 415–423, 1992.

[38] H. Nakano, S. Wakao, and T. Shimizu, "Correlation between crystal structure and electrochemical properties of C14 Laves-phase alloys," *J. Alloys Compd.*, vol. 253–254, pp. 609–612, May 1997.

[39] C. E. Lundin, F. E. Lynch, and C. B. Magee, "A correlation between the interstitial hole sizes in intermetallic compounds and the thermodynamic properties of the hydrides formed from those compounds," *J. Less-Common Met.*, vol. 56, no. 1, pp. 19–37, 1977.

[40] Y. Nakamura and E. Akiba, "H ydriding properties and crystal structure of NaCl-type mono-hydrides formed from Ti–V–Mn BCC solid solutions," *J. Alloys Compd.*, vol. 345, pp. 175–182, 2002.

[41] Z. Dehouche, M. Savard, F. Laurencelle, and J. Goyette, "Ti-V-Mn based alloys for hydrogen compression system," *J. Alloys Compd.*, vol. 400, no. 1–2, pp. 276–280, 2005.

[42] W. H. Hall, "X-Ray Line Broadening in Metals," *Proc. Phys. Soc.*, vol. 62, pp. 741–743, 1949.

[43] Z. Chen *et al.*, "Influence of Ti super-stoichiometry on the hydrogen storage properties of Ti1+xCr1.2Mn0.2Fe0.6 (x = 0-0.1) alloys for hybrid hydrogen storage application," *J. Alloys Compd.*, vol. 585, pp. 307–311, 2014.

[44] D. Fruchart, J. L. Soubeyroux, and R. Hempelmann, "Neutron diffraction in Ti1.2Mn1.8 deuteride: Structural and magnetic aspects," *J. Less Common Met.*, vol. 99, no. 2, pp. 307–319, 1984.

[45] K. Young, T. Ouchi, and M. A. Fetcenko, "Pressure-composition-temperature hysteresis in C14 Laves phase alloys: Part 3. Empirical formula," *J. Alloys Compd.*, vol. 480, no. 2, pp. 440–448, 2009.

8. Figures

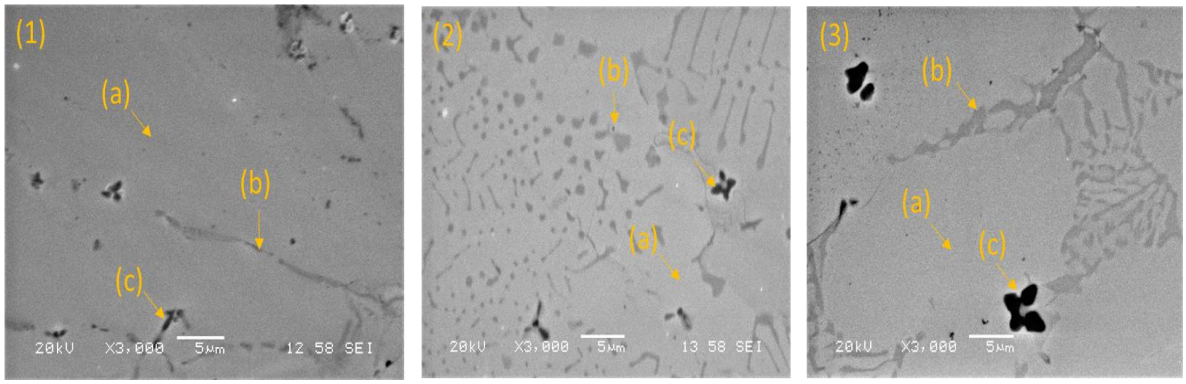

Figure 1: SEM Images of cross section of the (1) Alloy 1, (2) Alloy 2 and (3) Alloy 3 after synthesis. Various phases are shown by (a) the matrix phase, (b) the grey phase and (c) the dark phase.

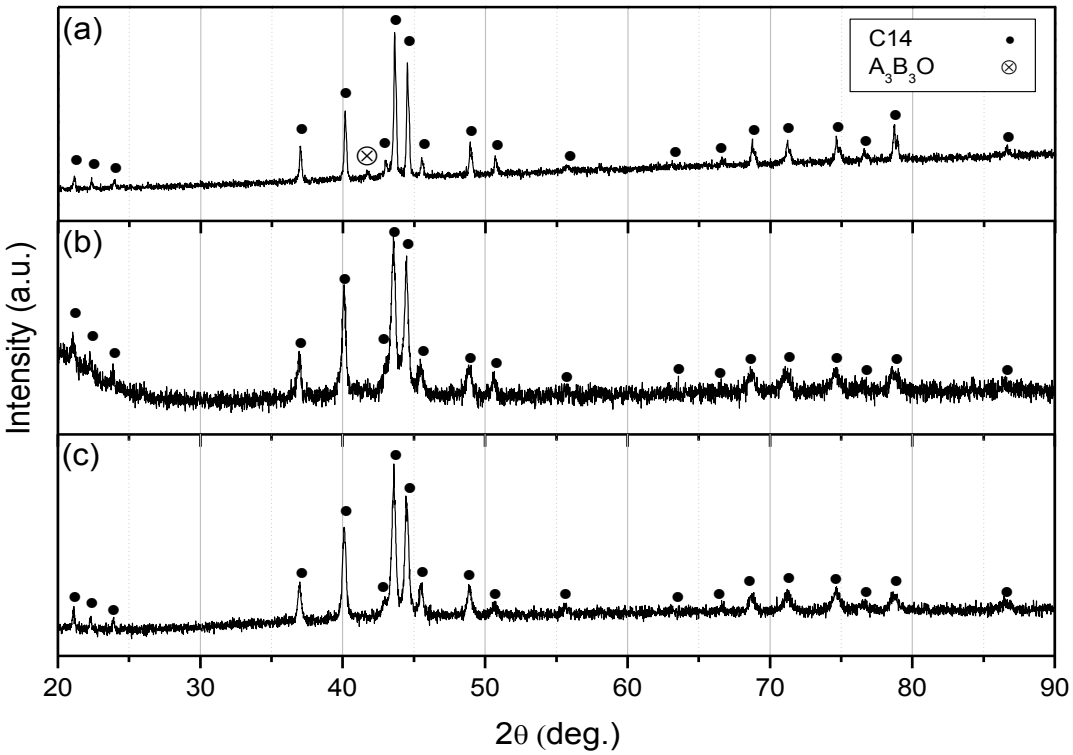

Figure 2: XRD patterns of the Alloy 1 (a) after synthesis (b) after hydrogen cycling (c) after heat treating of the cycled sample at 350 °C and 1 bar H_2.

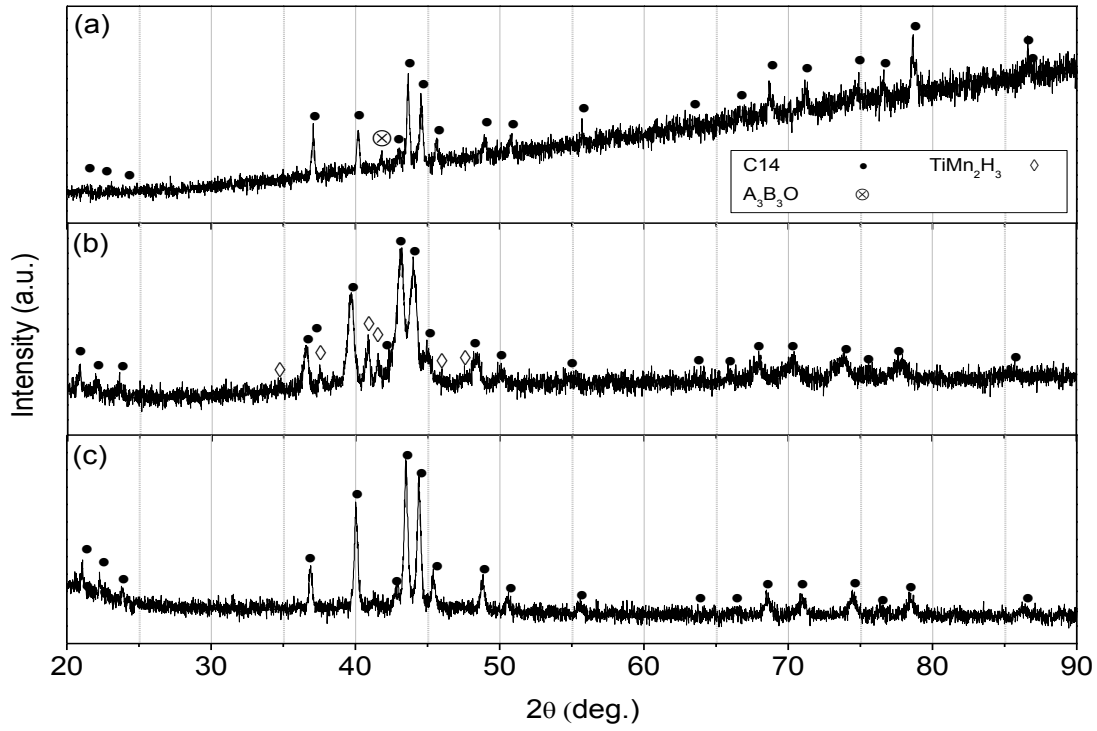

Figure 3: XRD patterns of the Alloy 2 (a) after synthesis (b) after hydrogen cycling (c) after heat treating of the cycled sample at 350 °C and 1 bar H_2.

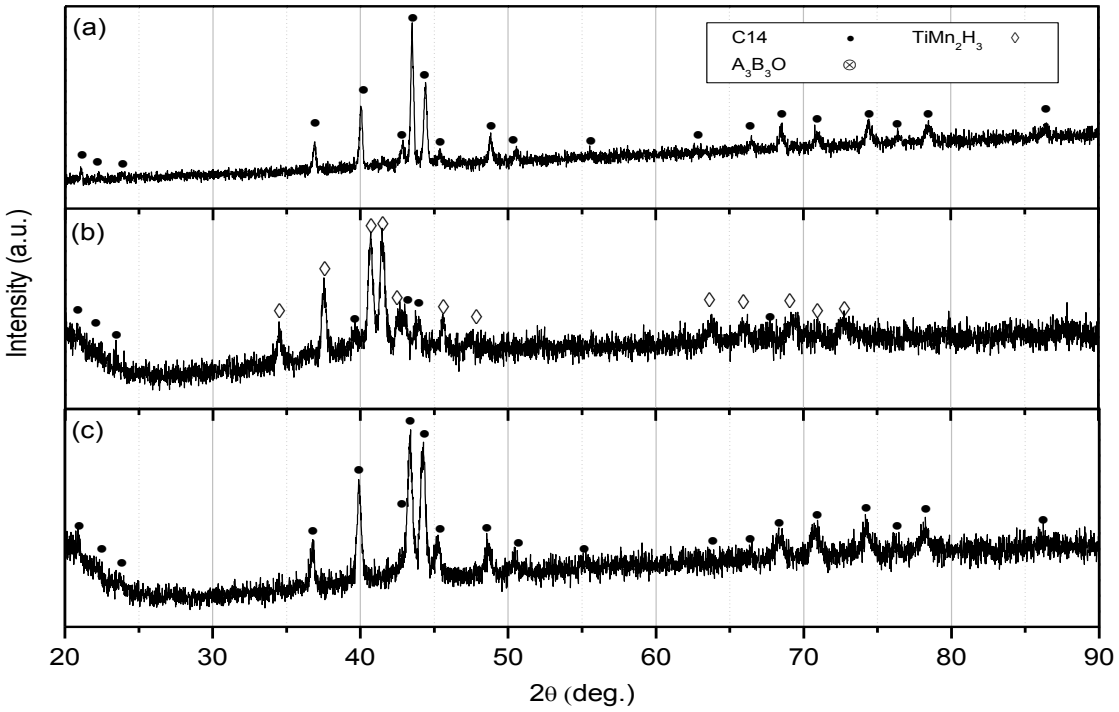

Figure 4: XRD patterns of the Alloy 3 (a) after synthesis (b) after hydrogen cycling (c) after heat treating of the cycled sample at 350 °C and 1 bar H_2.

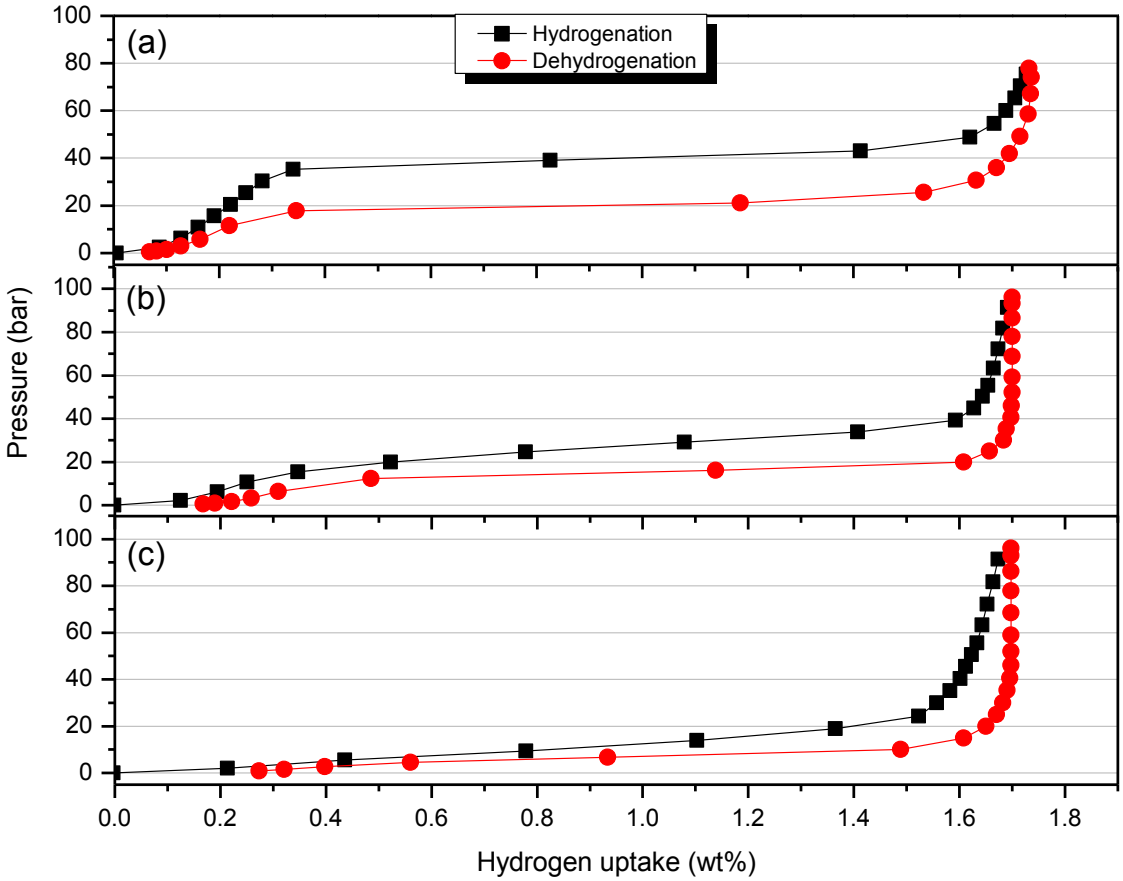

Figure 5: Room temperature PCI curves of the (a) Alloy 1 (b) Alloy 2 (c) Alloy 3

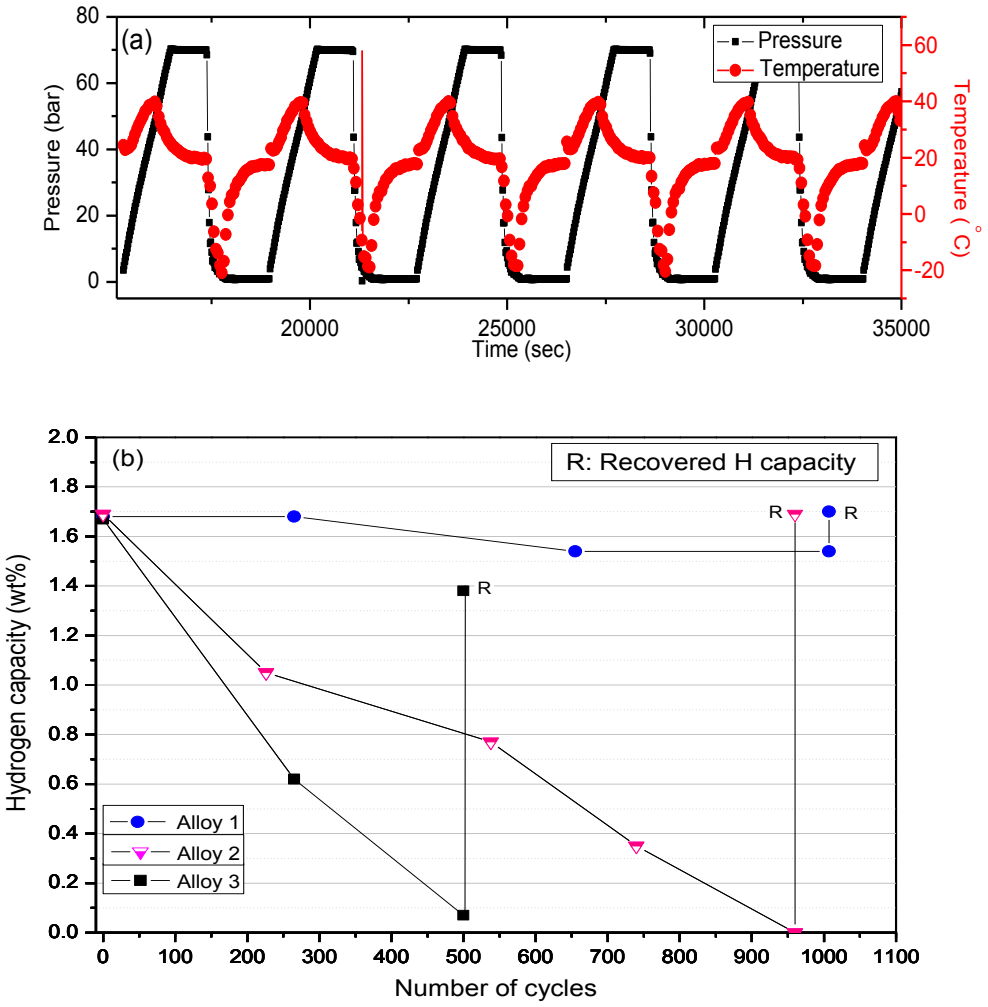

Figure 6: (a) Shows a few typical room temperature hydrogen cycles of the alloys. Complete hydrogenation and dehydrogenation are considered as a cycle, accompanied by exo/endothermic heat profile of the sample. (b) Shows in-situ measured changes in the hydrogen capacity of the alloys as a function of hydrogen cycles (solid lines are guide to the eye). R indicates the recovered hydrogen capacity of the cycled samples after the heat treatment at 350 °C and 1 bar H_2.

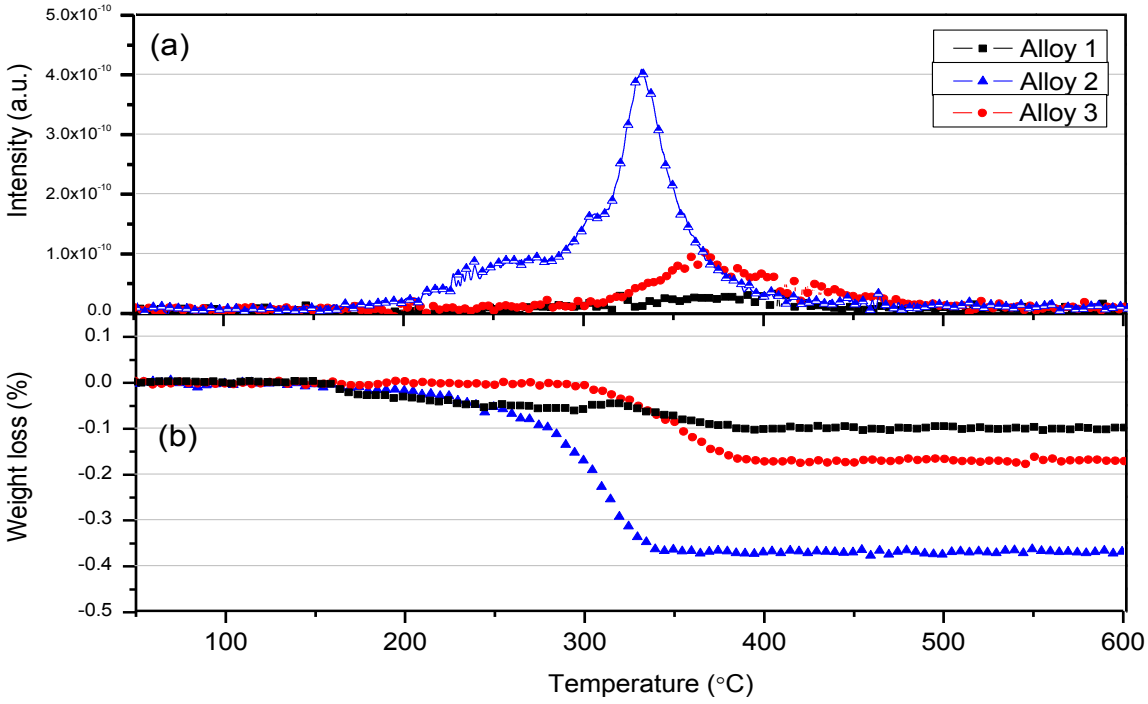

Figure 7: Thermal dehydrogenation profiles of the alloys after the hydrogen cycling. (a) Mass spectra (b) TG curves of the alloys.

9. Tables

Table 1: EDS compositional analysis for various phases of the alloys after synthesis (EDS errors within ±1 at. %)

Sample	EDS composition (at.%)	B:A atomic ratio
Alloy 1–matrix phase	$Ti_{30.6}V_{16.4}Mn_{48.7}(Zr_{0.7}Cr_{0.8}Fe_{2.8})$	2.19
Alloy 1-grey phase	$Ti_{41}V_{15.3}Mn_{39.3}(Zr_{1.5}Cr_{0.4}Fe_{2.5})$	1.35
Alloy 1-dark phase	$Ti_{54}V_{10.9}Mn_{29.6}(Zr_{3.6}Cr_{0.4}Fe_{1.5})$	0.74
Alloy 2-matrix phase	$Ti_{32.8}V_{15.1}Mn_{47.1}(Zr_{0.9}Cr_{1.2}Fe_{2.9})$	1.97
Alloy 2-grey phase	$Ti_{41.5}V_{13}Mn_{41.1}(Zr_{0.7}Cr_{0.7}Fe_{3})$	1.36
Alloy 2-dark phase	$Ti_{65.9}V_{9.2}Mn_{22.6}(Zr_{0.6}Cr_{0.2}Fe_{1.5})$	0.5
Alloy 3-matrix phase	$Ti_{34.5}V_{15.4}Mn_{44.7}(Zr_{0.9}Cr_{1.3}Fe_{3.2})$	1.82
Alloy 3- grey phase	$Ti_{44}V_{18.3}Mn_{34.3}(Zr_{0.5}Cr_{0.5}Fe_{2.4})$	1.24
Alloy 3-dark phase	$Ti_{88}V_{4.1}Mn_{6.9}(Zr_{0.6}Cr_{0.1}Fe_{0.3})$	0.12

Table 2: Phase abundance, lattice parameters and the C14 unit cell volumes of the alloys after synthesis (AS), after the cycling (C) and after the heat treating (HT), estimated by Rietveld refinement method. Included are also the crystalline size and heterogeneous strain of the alloys estimated by Hall's method.

Sample	Phase abundance (%)			*Mid plateau pressure (bar)**	*a* (nm)	*c* (nm)	*c/a*	C14 cell volume (nm^3)	Volume expansion** (%)	Crystalline size (nm)	Strain	Strain ratio***
	C14	FCC	TiMn Hx									
Alloy 1 - AS	~99	~1	-	Hy:39.5 Dehy:20.2	0.4865	0.7977	1.6396	0.1635	-	45.8	0.0049	-
Alloy 1 - C	100				0.4868	0.7980	1.6392	0.1638	0.17	29.5	0.0058	1.18
Alloy 1 - HT	100				0.4866	0.7979	1.6397	0.1636	0.09	31.07	0.0008	0.16
Alloy 2 - AS	92.3	7.7		Hy:26.2 Dehy:14.5	0.4871	0.7984	1.6390	0.1640	-	39.7	0.0127	-
Alloy 2 - C	86.5		13.5		0.4908	0.8047	1.6395	0.1679	2.32	21.2	0.0190	1.49
Alloy 2 - HT	100				0.4878	0.7996	1.6391	0.1647	0.42	33.06	0.0009	0.07
Alloy 3 - AS	100			Hy:11 Dehy:6.7	0.4879	0.7999	1.6394	0.1649	-	38.09	0.006	-
Alloy 3 - C	27.3		72.7		0.4936	0.8101	1.6412	0.1709	3.65	25.6	0.0202	3.37
Alloy 3 - HT	100				0.4889	0.8007	1.6377	0.1657	0.5	27.9	0.0113	1.9

* Hy: hydrogenation, Dehy: dehydrogenation.

** C14 cell volume expansion compared to the cell volume of the alloy after synthesis.

*** Heterogeneous strain compared to the heterogeneous strain of the alloy after synthesis.

Compositional effects on the h~~H~~ydrogen cycling stability of multicomponent Ti-Mn based alloys ~~as a function of stoichiometry~~

Shahrouz Nayebossadri and David Book
School of Metallurgy and Materials, University of Birmingham,
Edgbaston, Birmingham, B15 2TT, UK

Abstract

Intermetallic alloys such as AB, AB_2, and AB_5 type have been studied ~~as a form of~~ due to their capability to reversibly store hydrogen~~. storage~~. These a~~A~~lloys exhibit varying hydrogen storage properties depending on the crystal structure and composition. Compositional modification is commonly known as an effective method to modify the alloys thermodynamic and kinetics for various applications such as metal hydride batteries, metal hydrides hydrogen storage and compression. However, the effects of the compositional modification on the cyclic stability of these alloys are not usually well studied.

Here, the hydrogen cycling~~c~~ stabilities of Ti-Mn based alloys with C14 type structure are studied. Hyper-stoichiometry, stoichiometry and hypo-stoichiometry alloys were prepared accordingly: $Ti_{30.6}V_{16.4}Mn_{48.7}$ ($Zr_{0.7}Cr_{0.8}Fe_{2.8}$) (B/A=2.19), $Ti_{32.8}V_{15.1}Mn_{47.1}$ ($Zr_{0.9}Cr_{1.2}Fe_{2.9}$) (B/A=1.97) and $Ti_{34.5}V_{15.4}Mn_{44.7}$ ($Zr_{0.9}Cr_{1.3}Fe_{3.2}$) (B/A=1.87). Whilst the hyper-stoichiometry alloy showed almost a stable (about 9 % capacity reduction) hydrogen capacity after 1000 cycles of hydrogenation and dehydrogenation ~~ab/desorption~~, the stoichiometry and hypo-stoichiometry alloys failed to ~~absorb~~ hydrogenate after about 950 and 500 cycles respectively. ~~Heterogeneous strain and crystallite size of the alloys were calculated from the XRD pattern of the alloys after cyclic measurements.~~ A limited reduction in the calculated crystalline size of the alloys was observed before and after the hydrogen cycling, denoting that pulverisation plays a less significant role on the observed hydrogen capacity loss. ~~Only limited reduction in the crystalline size was observed~~, ~~denoting pulverisation plays a less significant role on the observed hydrogen capacity loss.~~ In addition, a reduction in the B/A ratio from 2.19 to 1.82 (hyper to hypo-stoichiometry) encouraged the formation of more stable hydride and a higher level of heterogeneous lattice strain. Whilst a small loss of hydrogen capacity (9%) in the hyper-stoichiometry alloy was attributed to the trapped hydrogen, the complete loss of hydrogen capacity in the stoichiometry and hypo-stoichiometry alloys seemed to originate from the formation of stable hydride and the lattice distortion.

~~hydride formation was only observed as the B/A ratio lowered which was accompanied by an increased level of heterogeneous strain. It seems that the loss of hydrogen capacity is mainly controlled by the level of retained hydrogen in the alloys interstitial sites and the hydride formation. Whilst accelerated loss in hydrogen capacity at lower B/A ratio may be~~

Formatted: Indent: First line: 0 cm

~~attributed to the hydride formation and the lattice distortion, a limited loss of hydrogen capacity at higher B/A ratio is mainly due to the trapped hydrogen.~~

Keywords: *Metal hydrides, Ti-Mn based alloys, C14 Laves phase, hydrogen cycling*

1. Introduction

The reversible reaction of some solid-state materials and hydrogen can offer a viable route to safely store, compress and transport hydrogen in a compact way [1], [2]. There are several metals and alloys capable to form hydrides at a range of pressures and temperatures [1]. Unlike ionic and covalent hydrides with a fixed composition, metal hydrides demonstrate high versatility in their composition, hence interesting materials for various applications [2], [3]. In particular, intermetallic compounds are promising materials for hydrogen storage due to their highly tunable properties. However, the stoichiometry of the intermetallic compound and therefore their crystal structure seems to dictate their hydrogen storage properties [2].

AB_2 intermetallic alloys based on the Laves phase crystal structures of cubic C15 (prototype $MgCu_2$, Pearson cF24 and space group *Fd*-3*m*) or hexagonal C14 (prototype $MgZn_2$, Pearson hP12, space group p63/*mmc*) have been studied for hydrogen storage [4]–[6]. Extended compositional homogeneity range can be offered by the Laves phase structure as a result of the vacancy formation, substitution of sub-stoichiometric atom positions by super-stoichiometric atoms in the structure and occupation of interstitial sites by super-stoichiometric atoms. [7], [8]. In addition, A and B elements can be easily replaced by additional alloying elements in most ~~Lavas~~ Laves phases [9], hence facilitating the modification of hydrogen storage properties of AB_2 intermetallic alloys.

Laves phase Ti-Mn based alloys are appealing hydrogen storage materials due to their acceptable hydrogen capacity at room temperature (~2wt%, suitable for stationary

applications), fast hydrogen ~~absorption~~ ation and ~~desorption~~ dehydrogenation kinetics, good cyclic stability, easy activation and a relatively low cost [10], [11]. However, the alloys composition and the type of substitutional elements can have a substantial effect on the hydrogen storage characteristics of the alloy. For instance, it was noted that hydrogen capacity and the cyclic stability of the alloy can be improved by increasing the volume fraction of $TiMn_2$ phase via keeping the Ti content of the alloy at an optimum level [12], [13]. The compositional dependent hydrogen storage properties have also led to numerous efforts for tuning the thermodynamic and kinetics of the Ti-Mn based alloys for specific applications by partially substituting A and B atoms with transitional metals ~~[10], [14]–[17]~~ [10], [14]–[18]. Nevertheless, besides the thermodynamic and kinetics improvements, other factors such as cyclic stability and sensitivity to gas impurities play an important role in the effective development of these alloys.

The effect of the pressure induced hy/dehydrogenation ~~ab/desorption~~ cycling on the performance of the $TiMn_{1.5}$, $Ti_{0.8}Zr_{0.2}Mn_{1.2}Mo_{0.1}$ and $Ti_{0.9}Zr_{0.1}Mn_{1.4}Cr_{0.4}V_{0.2}$ alloys were investigated [19]. The hydrogen capacity of the binary and multicomponent alloys were reduced by 30 % and 20 % respectively, after about 10000 cycles. Although cycling imposed lattice distortion, no stable hydride phase or phase disproportionation could be identified. The hydrogen capacity reduction was rather related to the surface poisoning by impurity gases. In another study [20], ~~a large reduction in the~~ hydrogen capacity of the $TiMn_2$ ($Ti_{40}Mn_{60}$ at. %) alloy almost halved (0.59 H/M to 0.3 H/M)~~occurred~~ after only 31 cycles. In this case, degradation in hydrogen capacity was attributed to the formation of stable Ti-H phase and retained hydrogen in interstitial sites accompanied by increasing lattice expansion and heterogeneous strain as a function of cycles. Yet, the hydrogen capacity in this alloy could be almost fully recovered by ~~appropriate~~ heating the alloy at 400 °C for 1 h

under argon. ~~treatment.~~ Compositional and structural changes in the C14 Laves phase were also held responsible for the loss of hydrogen capacity in Ti-Mn based alloys during cycling [21]. Whilst $Ti_{40}Mn_{60}$ alloy retained almost its full hydrogen capacity after 30 cycles, a slight change in the C14 Laves phase composition and therefore atomic site occupancy in the $Ti_{39}Mn_{61}$ (at. %) alloy could drastically decrease the cyclic stability.

The cyclic properties and effects of impurities in the gas stream on the hyper-stoichiometry $Ti_{0.98}Zr_{0.2}V_{0.43}Fe_{0.09}Cr_{0.05}Mn_{1.5}$ alloy were investigated [22] and only a limited degradation (less than 5 %) in the hydrogen capacity of the alloy was observed after 2000 cycles under high purity hydrogen (99.999%). However, the effects of gas impurities were distinct as N_2 and CH_4 only reduced the hydrogen ~~absorption~~ation kinetic, whereas O_2, CO, CO_2 and H_2O reduced the hydrogen capacity and cyclic stability of the alloy. It was especially noted that if O_2 presents higher than 0.03 wt % in the alloys, it can be detrimental to~~on~~ the formation of homogeneous microstructure of the Laves phase. Furthermore, long-term cyclic stability of the same alloy was studied under hydrogen (99.999 %) and no degradation in hydrogen capacity of the alloy was reported after 42400 cycles [23]. Cyclic stability of the $Ti_{0.98}Zr_{0.2}V_{0.43}Fe_{0.09}Cr_{0.05}Mn_{1.5}$ alloy was also examined [24] after ~~fabrication~~ synthesising with low-cost and low purity FeV and Ti sponge and only a limited reduction in hydrogen capacity occurred after 1000 cycles, similar to the alloy made from the high purity elements. Nevertheless, the importance of microstructural homogeneity to maintain the cyclic stability of AB_2 alloys is well established [12], [25]–[27].

Hence, it seems that the cyclic stability of Ti-Mn based alloys is controlled by the inherent properties of the alloys as well as the external factors. For example, thermodynamic preference of most intermetallic hydrides to form a stable elemental hydride can lead to a phase disproportionation and therefore reduced cyclic stability [28]. In the meantime, the

effect of experimental conditions such as hydrogen gas purity, temperature range, cycling repetition time, gas pressure and alloy's handling [29] are equally important on the cyclic lifetime of the alloys. Evaluation of the alloys cyclic lifetime may become challenging if the above factors are not examined systematically. In fact, most of the Laves phase AB_2 (particularly Ti-Mn based) alloys have been developed by compositional and structural modification for specific applications with limited attention to the cyclic stability of these alloys. ~~Here, we~~This work studies~~y~~ the effect of alloy~~'~~s stoichiometry on the cyclic stability of Ti-Mn based alloys under a similar experimental condition. The responsible mechanisms for hydrogen capacity loss and their relationship to the composition of alloys are investigated.

2. Experimental details

Three (hypo-stoichiometry, stoichiometry and hyper-stoichiometry) alloys were ~~fabricated~~ synthesised from elements. Elemental Ti (sponge, 99.95%), V (pieces, 99.7%), Mn (pieces, 99.9%), Zr (sponge 99.5%), Cr (pieces, 99.995%), Fe (pieces, 99.99%) and Ni (powder, 99 %) were purchased from Alfa Aesar. Alloys were pressed into pellets using an ATLAS automatic uniaxial press to produce a 2 g charge before ~~fabrication~~ synthesising by arc melting on a water-cooled copper crucible in an argon atmosphere. Remnant oxygen in the arc melting chamber was removed by melting a sacrificial oxygen getter before melting the alloys. The arc melting current was kept at 50 A to minimise the risk of losing elements during the arc strike. Each alloy was rotated and melted at least three times to ensure the homogeneity. No heat treatment was performed on the ~~fabricated~~ synthesised alloys and they were crushed to a particle size of less than 50 µm and kept inside an argon filled glove box.~~.~~

Alloys microstructure and composition were analysed by a Joel 6060 Scanning Electron Microscope (SEM) equipped with an INCA 300 Energy Dispersive Spectrometer (EDS). Alloys were mounted in Bakelite and polished with silicon carbide papers before final polishing

with OPA 1/4 micron suspension. Samples were cleaned using Acetone in a fume cupboard and dried with an electric hot air gun to avoid oxid~~is~~ation and surface pitting.

Room temperature X-Ray Diffraction (XRD) measurements were performed using a Bruker D8–Advanced diffractometer with monochromatic CuKα radiation (λ = 1.54056 Å). The XRD data was refined via a pseudo–Rietveld method with TOPAS Academic software [30] using published crystallographic information files (.cif) obtained from the Inorganic Crystal Systems Database [31].

Alloys were activated in-situ before Pressure Compositional Isotherm (PCI) measurement by heating the alloy to 300 °C and then admitting 100 bar H_2. Alloys were kept at this pressure for 4 h whilst cooling down to room temperature and vacuumed to approximately 10^{-6} mbar at the end of the sequence. The activation process was repeated at least three times for each sample to ensure a full activation. A volumetric Sieverts-type system (Hiden Isochema HTPS-2) was used for PCI measurements under high purity hydrogen (Air Products; BIP-Plus Hydrogen 99.99996 %). Before measurements, the sample volume was determined by helium pycnometry. PCI Measurements were performed between 0 and 100 bar H_2 at room temperature. Measurements were performed with a minimum holding time of 20 minutes to ensure no kinetic limitation for hy/dehydrogenation.

Room temperature cyclic hydrogen ~~ab/desorption~~ ation and dehydrogenation measurements ~~was~~ were performed on the activated alloys between 0 and 70 bar H_2 pressure (Air Products; BIP-Plus Hydrogen 99.99996 %) with a keeping time of 10 min at each pressure using another volumetric Sieverts-type system built by the Hydrogen Materials Group at the University of Birmingham. Sample temperature was monitored with a K-type thermocouple, directly in contact with the sample. Pressure transmitters (Maximum pressure of 200 bar) with an accuracy of ±0.25% were used to monitor changes

in the hydrogen pressure during hydrogen cycling. ~~-~~The cycled alloys were examined by XRD, Differential Scanning Calorimetry (Netzsch DSC 204 HP) and Thermal Gravimetric Analysis (Netzsch TG 209) coupled with a Hidden Analytical HAL IV Mass Spectrometry (MS). Approximately 30 mg of each alloy was loaded into TG/DSC and a heating rate of 2 °C/min and an Ar flow of 100 mL/min was applied.

Formatted: Font: Font color: Auto

Formatted: Indent: Left: 0 cm, First line: 0 cm

3. Results

3.1 Synthesised alloys

Elemental composition of the alloys was analysed by EDS and the results are given in Table 1. In addition, SEM micrographs of the alloys after ~~fabrication~~ synthesise are shown in Fig. 1. All the alloys can be characterised by a dominant matrix phase which is accompanied by minor grey and dark phases. Formation of the minority phases with different morphology in Ti-Mn based alloys have been reported [14], [15], [17], [21] which~~and it~~ seems to be controlled by the Ti and Mn content of the alloys. ~~Elemental composition of the alloys was analysed by EDS and the results are given in Table 1.~~ EDS results in Table 1 also indicate that all the alloys contain a small amount of other substitutional elements for A (Zr) and B (V, Fe, Cr) sites, which their quantities~~y is more or less similar in all~~do not significantly vary in the matrix phase of the alloys. However, the compositional analysis of the matrix phase shows a trend that is a reduction in Mn content and an increase in the Ti content ~~from Alloy 1 to Alloy 3~~of the alloys. As a result, a distinct B/A atomic ratio for each alloy can be seen in Table 1, ~~leading to the~~ formation ~~of~~ ng hyper-stoichiometry (Alloy 1), stoichiometry (Alloy 2) and hypo-stoichiometry (Alloy 3) alloys. The elemental composition of the minor grey and dark phases are also included in Table 1, revealing a higher Ti content at the~~i~~se regions, which is comparable to the previous studies [10], [14], [21]. Elemental composition of the grey phase shows a very close Ti and Mn content for all the alloys, hence denoting the

Formatted: No underline, Underline color: Auto, Pattern:

possible formation of TiMn phase. The volume fraction of the TiMn phase may be increased by decreasing the Mn content of the alloy. However, the formation of TiMn phase is not desireable as the hydrogen absorbed in this phase can be hardly desorbed [21]. The Ti content of the dark phase also seems to be significantly higher than the matrix phase, which can potentially lead to the formation of stable Ti-H phase during the cycling. The compositional variation in the grey and dark phases are also reflected by a significant reduction in their respecting B/A atomic ratio.

The XRD patterns for the Alloys 1, 2 and 3 after ~~fabrication~~ synthesise are given in Fig. 2a, 3a and 4a respectively. All the alloys contain $TiMn_2$ phase with a C14 Laves phase structure and no minority phases can be detected. The XRD patterns of the Alloy 1 and 2 also show the existence of η-carbide type oxide A_3B_3O phase (FCC structure) [32], [33], where A=Ti and Zr and B=Mn and V. Rietveld refinement results in Table 2 provides a phase abundance of FCC oxide phase as approximately 1 % and 7.7 % for the Alloy 1 and 2 respectively, whilst the Alloy 3 seems to be fully composed of C14 Laves phase. The oxide phase formation is mainly related to the alloys synthesis and handling processes, hence all the alloys were stored under an inert atmosphere to avoid a possible increase in the oxide content. In addition, the substitutional elements observed by EDS analysis in Table 1, could not encourage the formation of any new phases in the alloys. The capability of substitutional elements to occupy the atomic crystallographic positions of typical primary phase constituents creates a large structural homogeneity region in the C14 Laves phase [9], [34], [35]. This offers the opportunity to improve the hydrogen storage characteristics of the C14 Laves phase by partial elemental substitution [6], [36], [37].

Room temperature hy/dehydrogen ~~ab/desorption~~ ation PCI curves of the alloys are shown in Fig. 5. All the alloys show a single plateau for hy/dehydrogen ~~ab/desorption~~ ation with a

very similar maximum hydrogen capacity of approximately 1.7 %. The (mid) plateau pressures are highest for the Alloy 1 and lowest for the Alloy 3 (Table 2). The relationship is reversed in terms of C14 Laves phase unit cell volume of the alloys after the ~~fabrication~~ synthesis (Table 2), with the Alloy 1 possessing the smallest and the Alloy 3 the largest. The significant effect of C14 Laves phase unit cell volume on the thermodynamics of the AB_2 type alloys has been studied [38], [39] and it was revealed that there is a less favourable thermodynamic for hydride formation as the C14 Laves phase unit cell volume is reduced. In fact, ~~-~~thermodynamic properties of the Ti-Mn based alloys could be tuned for specific applications by altering the C14 Laves phase unit cell volumes through the modification of Ti and Mn content of the alloys [18] ~~we previously showed [39] the important role of the C14 Laves phase unit cell volumes for tuning the thermodynamic properties of the Ti-Mn based alloys for specific applications~~, ~~which could be primarily achieved by altering the Ti/Mn content of the alloys~~ [9], [35], [40], [41]. Also, the level of hysteresis seems to decrease from the Alloy 1 to the Alloy 3, whilst plateau slope increases. Although compositional modification ~~was identified [41] as~~seems to be an effective method to reduce the plateau slope in Ti-Mn base alloys, the level of hysteresis seemed to be mainly dictated by the thermodynamics of the alloy.

3.2 Cycled alloys

A typical cyclic measurement and the cyclic stability of the alloys under hydrogen are shown in Fig 6a and b. All the alloys were cycled under hydrogen between 0 and 70 bar whilst monitoring changes in the thermal profile of the samples showing exo/endotherms for hy/dehydrogenation respectively ~~ab/desorption~~ (Fig.6a). In-situ hydrogen capacity measurements were performed at specific points by disrupting the cyclic measurements (Fig 6b). The hydrogen capacity of the Alloy 1 appears to be stable until 250 cycles, where it

slowly starts to decrease (about 9 %) until 650 cycles and then becomes stable again up to over 1000 cycles. In contrast, Alloys 2 and 3 show a progressive reduction in their hydrogen capacity until the alloys fail to hydrogen ~~absorption~~ ate ~~is ceased~~ after 970 and 500 cycles respectively. Hydrogen capacity recovery was performed at the end of the cyclic measurements by heat treating the alloys under 1 bar hydrogen at 350 °C for 24 h. It seems that hydrogen capacity can be fully recovered for the Alloys 1 and 2, whereas the Alloy 3 only regains about 80 % of its original hydrogen capacity (Fig. 6b).

The XRD patterns of the cycled alloys are given in Fig. 2b, 3b and 4b. Alloy 1 preserves it's C14 Laves phase structure after the cycling (Fig. 2b), and the formation of any new phase/s cannot be observed. However, XRD patterns of the Alloys 2 and 3 signify the formation of stable $TiMn_2$ hydride phase along with their original C14 Laves phase (Fig 3b and 4b). The XRD patterns of the alloys after hydrogen capacity recovery (heat treated at 350 °C and 1 bar H_2) are given in Fig. 2c, 3c and 4c, indicating only the existence of C14 Laves phase. Structural refinement results in Table 2 provides a phase abundance of the hydrogen cycled and heat treated alloys. Whilst, Alloy 1 is entirely composed of C14 Laves phase, Alloys 2 and 3 show the formation of approximately 13.5 % and 72.7 % of stable $TiMn_2$ hydride phase respectively, along with their remaining C14 Laves phase. Nevertheless, the structures of the Alloys 2 and 3 can be fully reverted to the C14 Laves phase after the heat treatment (Fig. 3c and 4c).

The lattice parameters and the C14 Laves phase unit cell volume of the alloys after cycling and heat treatment are also listed in Table 2. The lattice parameters and therefore C14 Laves phase cell volume increase in all the alloys after hydrogen cycling. However, Alloy 1 shows the least volume expansion of 0.17 % compared to the much larger volume expansions of 2.32 % in the Alloy 2 and 3.65 % in the Alloy 3. It seems that the volume

expansions of C14 Laves phase remains to some extent in the Alloys 2 (0.42 %) and 3 (0.5 %) after the heat treatment, despite their full dehydrogenation as showed by XRD patterns in Fig. 3c and 4c. Minimal changes in the C14 unit cell volume of the Alloy 1 denotes a higher structural stability and the least changes in hydrogen absorptionation characteristics of the Alloy1 during hydrogen cycling.

XRD pattern of the C14 Laves phase in all the alloys also shows peak broadening after the hydrogen cycling. In general, XRD peak broadening after the hydrogen cycling can be attributed to a decrease in crytalline size and/or generation of heterogeneous strain [12], [21]. High density dislocation formation as a result of lattice parameters mismatch of the hydride phase and the alloy and retained hydrogen are proposed as the origin of heterogeneous strain during the cycling [20], [25], [27]. Crystalline size and the heterogeneous strain induced during the cycling can be estimated from Hall's method [20], [42]:

$$\frac{\beta \cos\theta}{\lambda} = 2\eta \frac{\sin\theta}{\lambda} + \frac{1}{\varepsilon} \quad (1)$$

Where β is the Full Width at Half Maximum Intensity (FWHMI), θ is the peak postion, λ is the wavelength of the x-ray (0.15405 nm), η is the hetrogeneous strain and ε is the crytalline size. Crystalline size and heterogeneus strain of the alloys were estimated from Eq. (1) and are listed in Table 2. The crystalline size for all the alloys decreases after the cycling and some limited regrowth in the crystalline size seems to occur after the heat treratment. Heterogeneous strain increases in all the alloys after the cycling but its magnitude is lowest for the Alloy 1 (given by stress ratio in Table 2) and highest for the Alloy 3. In addition, heat treatment seems to almost fully relief the heterogeneous strain in the Alloys 1 and 2, but the remained heterogeneous strain in the Alloy 3 is almost double the value of this alloy after the fabricationsynthesis.

~~5.~~ 4. Discussion

Formatted: No bullets or numbering

The observed unique cycling behaviour for each of the studied alloys signifies the important role of the alloy composition and structure on the cyclic lifetime. Although a relatively stable cyclic performance was reported for AB_2 type hydrides [21]–[24], The alloy composition seems to critically impact the cyclic property of the alloy. Here, the inherent properties of the alloys appear to be influenced as a result of a subtle change in the composition of the alloy. Degradation in ~~the~~ cyclic stability of the studied alloys could be occurred via pulverisation and/or phase disproportionation. The estimated crystalline size in Table 2, indicated a limited and nearly similar reduction in the crystalline size for all the alloys. Hence, the observed difference in the cyclic stability of the alloys is less likely to originate from the pulverisation. On the other hand, phase disproportionation could be seen in the Alloys 2 and 3 leading to the formation of stable hydride phase. In fact, it has been suggested that microstructural inhomogeneity as a result of changes in the alloys stoichiometry could potentially lead to disproportionation through the formation of stable hydride phases [27].

Dehydrogenation of the studied alloys was also investigated by TG-MS in Fig. 7. Surprisingly, hydrogen is also desorbed from the Alloy 1 (Fig. 7a), despite the lack of stable hydride phase after the cycling in this alloy (Fig.2b). TG curve of the Alloy 1 in Fig. 7b shows that the amount of released hydrogen is almost 0.1 wt %, which is close to the observed capacity loss of about 0.15 wt % at the end of the cycling (Fig. 6b). Although the proportion of the stable hydride phase in the Alloy 3 was higher compared to the Alloy 2 after the hydrogen cycling (Table 2), the amount of released hydrogen from the Alloy 2 (~0.4 wt %) is approximately twice the amount of hydrogen released from the Alloy 3 (~ 0.2 wt %) in ~~(~~Fig. 7b~~)~~. In addition, TG curves in Fig. 7b indicates that hydrogen is more loosely retained in the

Alloys 1 and 2 as ~~hydrogen starts to be desorbed~~the dehydrogenation starts at around ~~150~~ 180 °C compared to 300 °C for the Alloy 3.

The TG-MS data clearly indicate the effect of the retained hydrogen for capacity loss during the cycling. In fact, structural changes and deviation of Mn atomic position as a function of C14 Laves phase composition in Ti-Mn based alloys were observed [21] during hydrogen cycling. This could result in retained hydrogen inside the Laves phase which its scale gradually increased during the hydrogen cycling. The retained hydrogen was accompanied by heterogeneous strain and lattice expansion and its attenuating effect on hydrogen capacity was reported [18], [11], [25]. Hence, it seems that retained hydrogen, which is accompanied by a small increase in the lattice constants and C14 Laves phase volume, is the primary reason for the observed loss of hydrogen capacity in the Alloy 1. Nevertheless, hyper-stoichiometry of the Alloy 1 and its smaller C14 Laves phase cell volume seems to infer a higher cyclic stability at the beginning of the hydrogen cycling. Gradual changes in the C14 Laves phase structure (as evident from its lattice parameters and the cell volume) may lead to an increasing level of retained hydrogen that becomes noticeable ~~around~~ between 250 ~~cycles and saturates around~~to 650 cycles. Despite, the hydrogen interaction with the studied alloys during the cycling appears to be changing according to the alloys stoichiometry. Formation of stable hydride phase was observed in both Alloys 2 and 3 with lower B/A ratio (1.97 and 1.82 respectively) compared to the Alloy 1 (2.19) after the hydrogen cycling. Extended compositional homogeneity range in C14 Laves phase implies considerable changes in certain atomic and interstitial site occupation may occur as a result~~s~~ of changes in the composition of the alloy. Compositional changes may encourage the formation of interstitial sites with different local chemical environments. For example, the introduction of Ti into the B sites can create a series of interstitial sites rich in Ti, showing

different affinities to hydrogen [43]. It was shown that [44] the excess Ti atoms in $Ti_{1.2}Mn_{1.8}$ alloy occupy one of the Mn atomic positions, preferably *2a* sites, leading to the formation of the Ti_3Mn interstitial site with high hydrogen affinity. Increasing the Ti content in the multicomponent alloys were also noted to enhance the alloy-hydrogen interaction [13]. The hydrogen ~~absorption~~ation plateau pressures of the studied alloys lowered ~~(Fig. 5)~~ as the B/A ratio decreased (Fig. 5 and Table 1), indicating a more favourable thermodynamic for hydride formation. This was reflected in the higher phase abundance of the formed stable hydrides in the Alloys 3 (72.7 %) compared to the Alloy 2 (13.5 %), in accordance with their Ti content. However, a higher amount of hydrogen desorbed from the Alloy 2 compared to the Alloy 3 after the hydrogen cycling (Fig. 7b) may also be ~~also~~ attributed to the contribution of retained hydrogen in the lattice rather than just dehydrogenation of the stable hydride phase. This can be corroborated by the similar dehydrogenation onset temperature (~ 180 °C) of the Alloy 2 to the Alloy 1 with no sign of stable hydride formation after the hydrogen cycling. In contrast, dehydrogenation of the Alloy 3 starts at a higher temperature (~ 300 °C) which may be entirely attributed to the dehydrogenation of the stable hydride phase observed after the hydrogen cycling. It is worth mentioning that the level of the hydrogen released from the Alloy 2 and especially Alloy 3 with a higher hydride phase abundance is well below the observed ~~alloys~~ maximum hydrogen capacity of the alloys (~ 1.7 wt %). This may suggest~~s~~ that the stable hydrides are ~~mainly~~ predominantly formed on the surface of the alloys, which could kinetically inhibit hy/dehydrogenation of the alloys at the studied experimental conditions.

Also, it was shown in Fig. 6b that the hydrogen capacity could be only fully recovered in the Alloys 1 and 2 after the heat treatment. Although heat treatment completely reverts the structure of the Alloys 2 and 3 to C14 Laves phase (Table 2), the volume expansion of the

Alloys 2 and 3 remains at 0.42 % and 0.5 % respectively. Furthermore, unlike the Alloy 2 which its volume expansion does not lead to an increased heterogeneous strain ratio, the volume expansion in the Alloy 3 is accompanied by a higher heterogeneous strain ratio compared to this alloy after the synthesis~~fabrication~~. This may be explained by the variation of *c/a* ratio of the C14 Laves phase as given in Table 2. The *c/a* ratio of the Alloy 2 after heat treatment is almost similar to the original value after the ~~fabrication~~synthesis. In contrast, the *c/a* ratio of the Alloy 3 after the heat treatment is considerably smaller compared to its value after the ~~fabrication~~synthesis, denoting a non-uniform hexagonal cell expansion along the *a* axis. It is known that [45] C14 Laves phase can be permanently deformed as a result of variation in its lattice parameters when interacting with hydrogen. It may be suggested that the higher level of hydride formed in the Alloy 3 deformed the C14 laves phase structure (e.g. by escalated dislocation density). Hence, the observed structural changes in the Alloy 3 may be responsible for the lack of full hydrogen capacity recovery after the heat treatment.

Overall, the observed loss of capacity during hydrogen cycling in the studied alloys appears to be a dynamic process, dominated by the alloy stoichiometry. Nevertheless, the cyclic stability of the alloys, particularly those with low hydrogen ~~absorption~~ation plateau pressure, may be extended by tuning the experimental condition.

~~6.~~5. Conclusions

The effects of small stoichiometric changes on the microstructure, hydrogenation ~~absorption~~ characteristics and particularly cyclic stability of the Ti-Mn based multicomponent alloys were investigated. The microstructure of hyper-stoichiometry (Alloy 1), stoichiometry (Alloy 2) and hypo-stoichiometry alloys featured a main C14 Laves phase accompanied by small secondary phases with considerably higher Ti contents. The hydrogenation ~~absorption~~ characteristics of the alloys changed ~~as a function of~~with respects

to the alloys stoichiometry. Lowering B/A ratio reduced the hydrogen ~~absorption~~ation plateau pressure. Cyclic stabilities of the alloys under high purity hydrogen were studied and hyper-stoichiometric alloy showed only about 9 % reduction in its hydrogen storage capacity after 1000 cycles as opposed to the full hydrogen capacity loss after about 950 cycles in the stoichiometry and about 500 cycles in the hypo-stoichiometry alloys. The loss of hydrogen capacity seemed to be caused by the retained hydrogen in C14 Laves phase lattice and/or the formation of stable hydride phase. However, this is a dynamic mechanism which suggested to be mainly determined by the composition of the alloy and to a lower extent by the experimental conditions, especially for the alloys with low hydrogenation ~~absorption~~ plateau pressures. Nevertheless, hydride formation during the cycling may cause levels of irreversible hydrogen capacity loss by gradually degrading the C14 Laves phase structure.

~~7.~~6. Acknowledgments

Support from the EPSRC Engineering Safe and Efficient Hydride-based Technologies (EP/K021117/1) and STFC Early Career Award (ST/N002385/1) is gratefully acknowledged. Authors would like to thank Professor David Grant, Professor Gavin Walker and Dr. Alastair Stuart for their support and guidance.

7. References

Formatted: Font: Bold

Formatted: List Paragraph, Space After: 0 pt, Line spacing: single, Numbered + Level: 1 + Numbering Style: 1, 2, 3, … + Start at: 5 + Alignment: Left + Aligned at: 0 cm + Indent at: 0.63 cm

[1] D. F. Shriver and P. W. Atkins, *Inorganic Chemistry*, 3rd ed. London W. H. Freeman & Co, 1999.

[2] G. Sandrock, "A panoramic overview of hydrogen storage alloys from a gas reaction point of view," *J. Alloys Compd.*, vol. 293–295, pp. 877–888, Dec. 1999.

[3] N. A. A. Rusman and M. Dahari, "A review on the current progress of metal hydrides material for solid-state hydrogen storage applications," *Int. J. Hydrogen Energy*, vol. 41, no. 28, pp. 12108–12126, 2016.

[4] K. Young, T. Ouchi, J. Yang, and M. A. Fetcenko, "Studies of off-stoichiometric AB2 metal hydride alloy: Part 1. Structural characteristics," *Int. J. Hydrogen Energy*, vol. 36, no. 17, pp. 11137–11145, 2011.

[5] K. Young, J. Nei, B. Huang, and M. A. Fetcenko, "Studies of off-stoichiometric AB2 metal hydride alloy: Part 2. Hydrogen storage and electrochemical properties," *Int. J. Hydrogen Energy*, vol. 36, no. 17, pp. 11146–11154, 2011.

[6] K. Manickam, D. M. Grant, and G. S. Walker, "Optimization of AB2 type alloy composition with superior hydrogen storage properties for stationary applications," *Int. J. Hydrogen Energy*, vol. 40, no. 46, pp. 16288–16296, 2015.

[7] N. A. Kelly and R. Girdwood, "Evaluation of a thermally-driven metal-hydride-based hydrogen compressor," *Int. J. Hydrogen Energy*, vol. 37, no. 14, pp. 10898–10916, Jul. 2012.

[8] P. Muthukumar, M. Prakashmaiya, and S. Srinivasamurthy, "Experiments on a metal hydride based hydrogen compressor," *Int. J. Hydrogen Energy*, vol. 30, no. 8, pp. 879–892, Jul. 2005.

[9] S. V. Mitrokhin, "Regularities of hydrogen interaction with multicomponent Ti(Zr)–Mn–V Laves phase alloys," *J. Alloys Compd.*, vol. 404–406, pp. 384–387, Dec. 2005.

[10] M. Shibuya, J. Nakamura, and E. Akiba, "Hydrogenation properties and microstructure of Ti-Mn-based alloys for hybrid hydrogen storage vessel," *J. Alloys Compd.*, vol. 466, no. 1–2, pp. 558–562, 2008.

[11] B.-H. Liu, D.-M. Kim, K.-Y. Lee, and J.-Y. Lee, "Hydrogen storage properties of TiMn2-based alloys," *J. Alloys Compd.*, vol. 240, no. 1–2, pp. 214–218, 1996.

[12] S. Semboshi, N. Masahashi, and S. Hanada, "Effect of composition on hydrogen absorbing properties in binary TiMn2based alloys," *J. Alloys Compd.*, vol. 352, no. 1–2, pp. 210–217, 2003.

[13] T. Gamo and Y. Moriwaki, "Formation and properties of titanium-manganese alloy hydrides," *Int. J. Hydrogen Energy*, vol. 1, no. 1, pp. 39–47, 1985.

[14] M. Au, F. Pourarian, S. G. Sankar, W. E. Wallace, and L. Zhang, "TiMn2-based alloys as high hydrogen storage materials," *Mater. Sci. Eng. B*, vol. 33, pp. 53–57, 1995.

[15] X. Yu, B. Xia, Z. Wu, and N. Xu, "Phase structure and hydrogen sorption performance of Ti-Mn-based alloys," *Mater. Sci. Eng. A*, vol. 373, no. 1–2, pp. 303–308, 2004.

[16] M. . Hagström, J. . Vanhanen, and P. . Lund, "AB2 metal hydrides for high-pressure and narrow temperature interval applications," *J. Alloys Compd.*, vol. 269, no. 1–2, pp. 288–293, 1998.

[17] L. Pickering, D. Reed, A. I. Bevan, and D. Book, "Ti-V-Mn based metal hydrides for hydrogen compression applications," *J. Alloys Compd.*, vol. 645, no. S1, pp. S400–S403, 2015.

[18] R. R. Chen *et al.*, "Effects of Ti/Mn ratio on microstructure and hydrogen storage properties of Ti-V-Mn alloys," *J. Alloys Compd.*, vol. 748, pp. 171–178, 2018.

[19] T. Gamo, Y. Moriwaki, N. Yanagihara, and T. Iwaki, "Life properties of TiMn alloy hydrides and their hydrogen purification effect," *J. Less-Common Met.*, vol. 89, no. 2, pp. 495–504, 1983.

[20] S. Semboshi, N. Masahashi, and S. Hanada, “Degradation of hydrogen absobing capacity in cyclically hydrogenated TiMn2,” *Acta Mater.*, vol. 49, no. 5, pp. 927–935, 2001.

[21] S. Semboshi, M. Sakurai, N. Masahashi, T. J. Konno, and S. Hanada, “Effect of structural changes on degradation of hydrogen absorbing capacity in cyclically hydrogenated TiMn2based alloys,” *J. Alloys Compd.*, vol. 376, no. 1–2, pp. 232–240, 2004.

[22] D. Bernauer, O. Topler, J. Noresus, D. Hempelmann, R. Richter, “F U N D A M E N T A L S A N D PROPERTIES OF SOME Ti/Mn BASED LAVES PHASE HYDRIDES 0 .,” *Int. J. Hydrogen Energy*, vol. 14, no. 3, pp. 187–200, 1989.

[23] G. Friedlmeier, A. Manthey, M. Wanner, and M. Groll, “Cyclic stability of various application-relevant metal hydrides,” *J. Alloys Compd.*, vol. 231, no. 1–2, pp. 880–887, 1995.

[24] U. Ulmer, M. Dieterich, A. Pohl, R. Dittmeyer, M. Linder, and M. Fichtner, “Study of the structural, thermodynamic and cyclic effects of vanadium and titanium substitution in laves-phase AB2hydrogen storage alloys,” *Int. J. Hydrogen Energy*, vol. 42, no. 31, pp. 20103–20110, 2017.

[25] V. Iosub, J. M. Joubert, M. Latroche, R. Cerný, and A. Percheron-Guégan, “Hydrogen cycling induced diffraction peak broadening in C14 and C15 Laves phases,” *J. Solid State Chem.*, vol. 178, no. 6, pp. 1799–1806, 2005.

[26] Y. Zhu, H. Pan, M. Gao, Y. Liu, and Q. Wang, “A study on improving the cycling stability of (Ti0.8Zr0.2)(V0.533Mn0.107Cr0.16Ni0.2)4 hydrogen storage electrode alloy by means of annealing treatment: I: Effects on the structures,” *J. Alloys Compd.*, vol. 347, pp. 279–284, 2002.

[27] S. Selvaraj *et al.*, “Study of cyclic performance of V-Ti-Cr alloys employed for hydrogen compressor,” *Int. J. Hydrogen Energy*, pp. 1–9, 2018.

[28] G. D. Sandrock and P. D. Goodell, “Cyclic life of metal hydrides with impure hydrogen: Overview and engineering considerations,” *J. Less-Common Met.*, vol. 104, no. 1, pp. 159–173, 1984.

[29] R. C. Bowman, C. H. Luo, C. C. Ahn, C. K. Witham, and B. Fultz, “The effect of tin on the degradation of LaNi5-ySny metal hydrides during thermal cycling,” *J. Alloys Compd.*, vol. 217, no. 2, pp. 185–192, 1995.

[30] A. Coelho, “Topas-Academic, Version 4.1, Coelho Software, Brisbane, Australia,” 2007.

[31] D. A. Fletcher, R. F. McMeeking, and D. Parkin, “The United Kingdom Chemical Database Service,” *J. Chem. Inf. Model.*, vol. 36, no. 4, pp. 746–749, 1996.

[32] J. Huot, E. Akiba, and Y. Ishido, “Crystal structure of multiphase alloys (Zr, Ti)(Mn, V) 2,” *J. Alloys Compd.*, vol. 231, pp. 85–89, 1995.

[33] M. Shibuya, J. Nakamura, H. Enoki, and E. Akiba, “High-pressure hydrogenation properties of Ti–V–Mn alloy for hybrid hydrogen storage vessel,” *J. Alloys Compd.*, vol. 475, no. 1–2, pp. 543–545, May 2009.

[34] S. . Mitrokhin, T. . Bezuglaya, and V. . Verbetsky, “Structure and hydrogen sorption properties of (Ti,Zr)–Mn–V alloys,” *J. Alloys Compd.*, vol. 330–332, pp. 146–151, 2002.

[35] S. V Mitrokhin, T. N. Smirnova, V. A. Somenkov, V. P. Glazkov, and V. N. Verbetsky, “Structure of (Ti,Zr)-Mn-V nonstoichiometric Lavas phases and (Ti0.9Zr0.1)(Mn0.75V0.15Ti0.1D2.8 deuteride,” *J. Alloys Compd.*, vol. 357, pp. 80–83, 2003.

[36] J. L. Bobet, B. Chevalier, and B. Darriet, “Crystallographic and hydrogen sorption properties of TiMn2 based alloys,” *Intermetallics*, vol. 8, no. 4, pp. 359–363, 2000.

[37] J. D. Livingston, “Laves-phase superalloys?,” *Phys. Status Solidi*, vol. 131, no. 2, pp. 415–423, 1992.

[38] H. Nakano, S. Wakao, and T. Shimizu, “Correlation between crystal structure and electrochemical properties of C14 Laves-phase alloys,” *J. Alloys Compd.*, vol. 253–254, pp. 609–612, May 1997.

[39] C. E. Lundin, F. E. Lynch, and C. B. Magee, “A correlation between the interstitial hole sizes in intermetallic compounds and the thermodynamic properties of the hydrides formed from those compounds,” *J. Less-Common Met.*, vol. 56, no. 1, pp. 19–37, 1977.

[40] Y. Nakamura and E. Akiba, “H ydriding properties and crystal structure of NaCl-type mono-hydrides formed from Ti–V–Mn BCC solid solutions,” *J. Alloys Compd.*, vol. 345, pp. 175–182, 2002.

[41] Z. Dehouche, M. Savard, F. Laurencelle, and J. Goyette, “Ti-V-Mn based alloys for hydrogen compression system,” *J. Alloys Compd.*, vol. 400, no. 1–2, pp. 276–280, 2005.

[42] W. H. Hall, “X-Ray Line Broadening in Metals,” *Proc. Phys. Soc.*, vol. 62, pp. 741–743, 1949.

[43] Z. Chen *et al.*, “Influence of Ti super-stoichiometry on the hydrogen storage properties of Ti1+xCr1.2Mn0.2Fe0.6 (x = 0-0.1) alloys for hybrid hydrogen storage application,” *J. Alloys Compd.*, vol. 585, pp. 307–311, 2014.

[44] D. Fruchart, J. L. Soubeyroux, and R. Hempelmann, “Neutron diffraction in Ti1.2Mn1.8 deuteride: Structural and magnetic aspects,” *J. Less Common Met.*, vol. 99, no. 2, pp. 307–319, 1984.

[45] K. Young, T. Ouchi, and M. A. Fetcenko, “Pressure-composition-temperature hysteresis in C14 Laves phase alloys: Part 3. Empirical formula,” *J. Alloys Compd.*, vol. 480, no. 2, pp. 440–448, 2009.

8. Figures

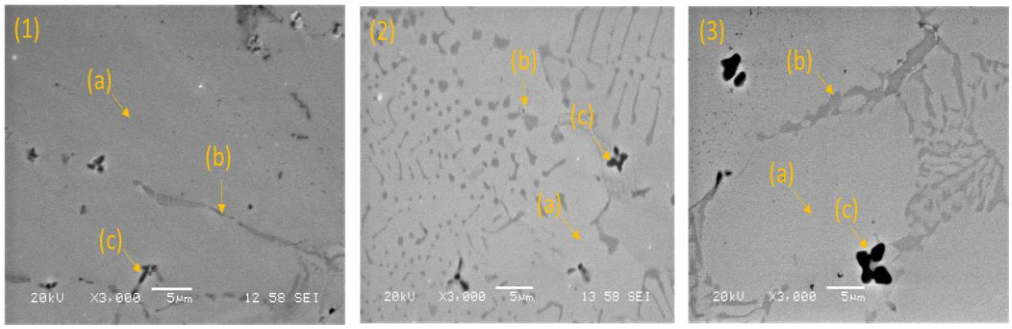

Figure 1: SEM Images of cross section of the (1) Alloy 1, (2) Alloy 2 and (3) Alloy 3 after ~~the fabrication~~synthesis. Various phases are shown by (a) the matrix phase, (b) the grey phase and (c) the dark phase.

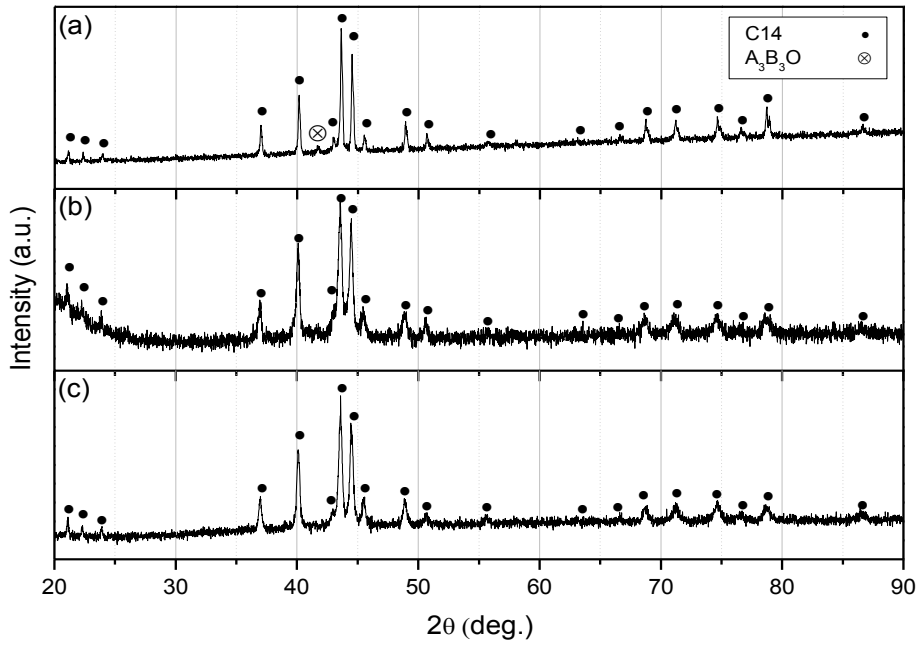

Figure 2: XRD patterns of the Alloy 1 (a) after synthesis ~~fabrication~~ (b) after hydrogen cycling (c) after heat treating of the cycled sample at 350 °C and 1 bar H_2.

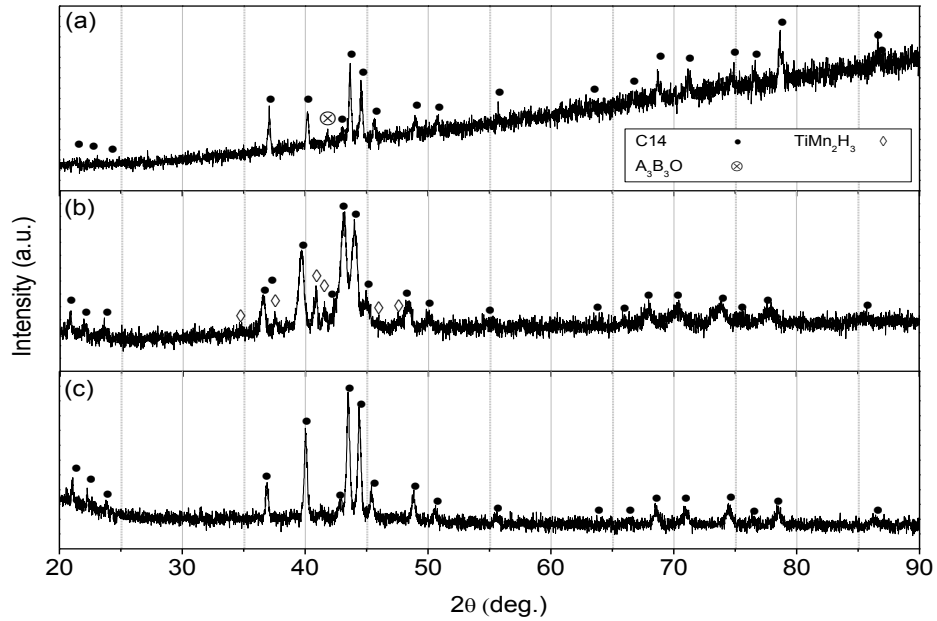

Figure 3: XRD patterns of the Alloy 2 (a) after ~~fabrication~~ synthesis (b) after hydrogen cycling (c) after heat treating of the cycled sample at 350 °C and 1 bar H_2.

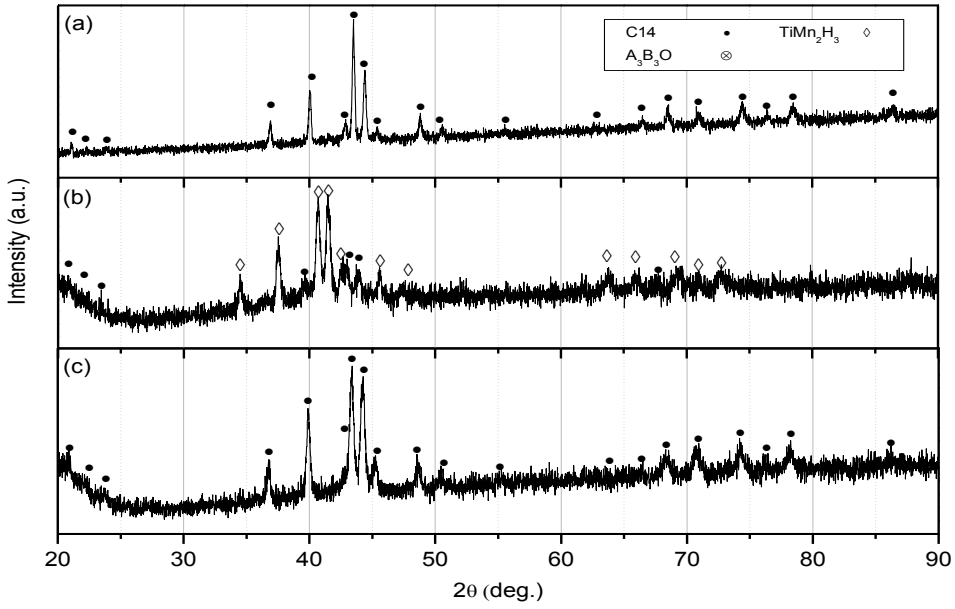

Figure 4: XRD patterns of the Alloy 3 (a) after ~~fabrication~~ synthesis (b) after hydrogen cycling (c) after heat treating of the cycled sample at 350 °C and 1 bar H_2.

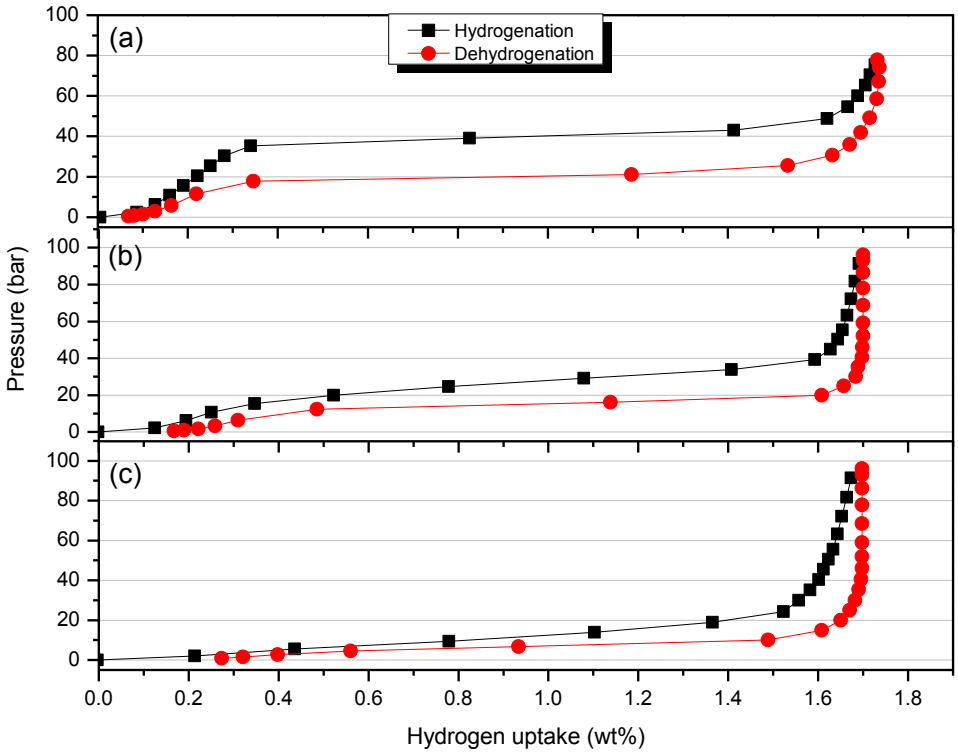

Figure 5: Room temperature PCI curves of the (a) Alloy 1 (b) Alloy 2 (c) Alloy 3

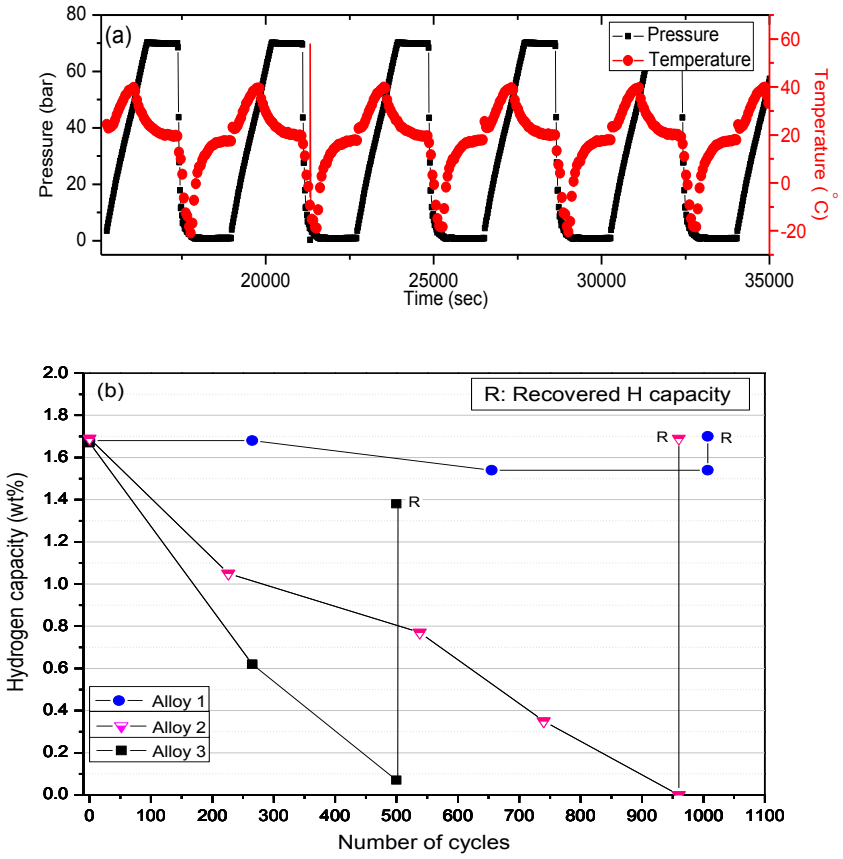

Figure 6: (a) Shows a few typical room temperature hydrogen cycles of the alloys. A complete hydrogen ~~absorption and desorption~~ ation and dehydrogenation are considered as a cycle, accompanied by exo/endothermic heat profile of the sample. (b) Shows in-situ measured changes in the hydrogen capacity of the alloys as a function of hydrogen cycles (solid lines are guide to the eye). R indicates the recovered hydrogen capacity of the cycled samples after the heat treatment at 350 °C and 1 bar H_2.

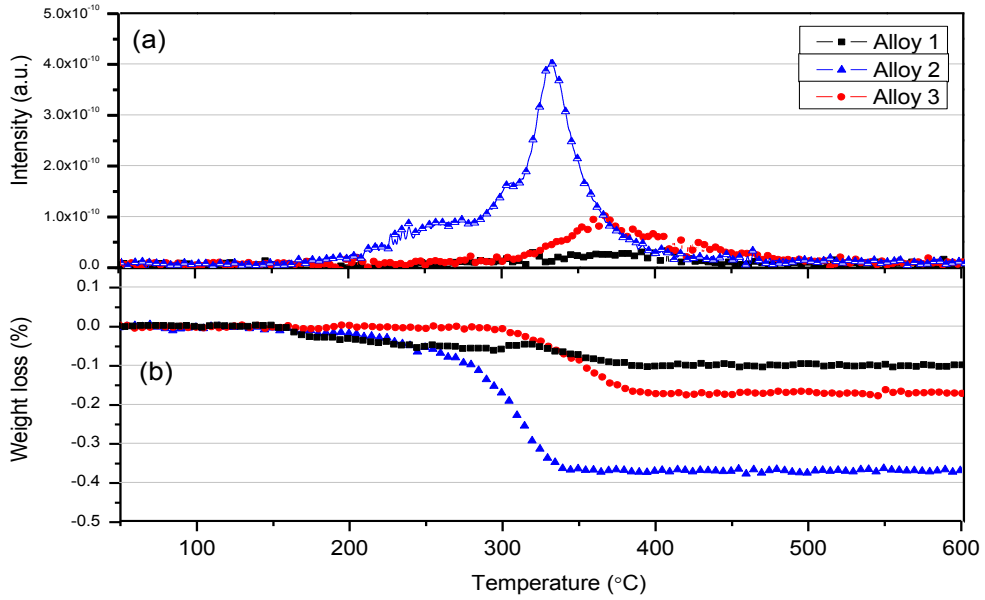

Figure 7: Thermal ~~desorption~~ dehydrogenation profiles of the alloys after the hydrogen cycling. (a) Mass spectra (b) TG curves of the alloys.

9. Table

Table 1: EDS compositional analysis for various phases of the alloys after ~~fabrication~~ synthesis (EDS errors within ±1 at. %)

Sample	EDS composition (at.%)	B:A atomic ratio
Alloy 1–matrix phase	$Ti_{30.6}V_{16.4}Mn_{48.7}(Zr_{0.7}Cr_{0.8}Fe_{2.8})$	2.19
Alloy 1-grey phase	$Ti_{41}V_{15.3}Mn_{39.3}(Zr_{1.5}Cr_{0.4}Fe_{2.5})$	1.35
Alloy 1-dark phase	$Ti_{54}V_{10.9}Mn_{29.6}(Zr_{3.6}Cr_{0.4}Fe_{1.5})$	0.74
Alloy 2-matrix phase	$Ti_{32.8}V_{15.1}Mn_{47.1}(Zr_{0.9}Cr_{1.2}Fe_{2.9})$	1.97
Alloy 2-grey phase	$Ti_{41.5}V_{13}Mn_{41.1}(Zr_{0.7}Cr_{0.7}Fe_{3})$	1.36
Alloy 2-dark phase	$Ti_{65.9}V_{9.2}Mn_{22.6}(Zr_{0.6}Cr_{0.2}Fe_{1.5})$	0.5
Alloy 3-matrix phase	$Ti_{34.5}V_{15.4}Mn_{44.7}(Zr_{0.9}Cr_{1.3}Fe_{3.2})$	1.82
Alloy 3- grey phase	$Ti_{44}V_{18.3}Mn_{34.3}(Zr_{0.5}Cr_{0.5}Fe_{2.4})$	1.24
Alloy 3-dark phase	$Ti_{88}V_{4.1}Mn_{6.9}(Zr_{0.6}Cr_{0.1}Fe_{0.3})$	0.12

Formatted: Font: (Default) Calibri, Bold

Formatted: List Paragraph, Indent: Left: 0 cm, Hanging: 0.5 cm, Space After: 0 pt, Line spacing: single, Numbered + Level: 1 + Numbering Style: 1, 2, 3, … + Start at: 9 + Alignment: Left + Aligned at: 0.63 cm + Indent at: 1.27 cm

Table 2: Phase abundance, lattice parameters and the C14 unit cell volumes of the alloys after ~~fabrication~~ synthesis (AS~~F~~), after the cycling (C) and after the heat treating (HT), estimated by Rietveld refinement method. Included are also the crystalline size and heterogeneous strain of the alloys estimated by Hall's method.

Sample	Phase abundance (%)			*Mid plateau pressure (bar)**	*a* (nm)	*c* (nm)	*c/a*	C14 cell volume (nm^3)	Volume expansion** (%)	Crystalline size (nm)	Strain	Strain ratio***
	C14	FCC	TiMn Hx									
Alloy 1 - AS~~F~~	~99	~1	-	Hy:39.5 Dehy:20.2	0.4865	0.7977	1.6396	0.1635	-	45.8	0.0049	-
Alloy 1 - C	100				0.4868	0.7980	1.6392	0.1638	0.17	29.5	0.0058	1.18
Alloy 1 - HT	100				0.4866	0.7979	1.6397	0.1636	0.09	31.07	0.0008	0.16
Alloy 2 - AS~~F~~	92.3	7.7		Hy:26.2 Dehy:14.5	0.4871	0.7984	1.6390	0.1640	-	39.7	0.0127	-
Alloy 2 - C	86.5		13.5		0.4908	0.8047	1.6395	0.1679	2.32	21.2	0.0190	1.49
Alloy 2 - HT	100				0.4878	0.7996	1.6391	0.1647	0.42	33.06	0.0009	0.07
Alloy 3 - AS~~F~~	100			Hy:11 Dehy:6.7	0.4879	0.7999	1.6394	0.1649	-	38.09	0.006	-
Alloy 3 - C	27.3		72.7		0.4936	0.8101	1.6412	0.1709	3.65	25.6	0.0202	3.37
Alloy 3 - HT	100				0.4889	0.8007	1.6377	0.1657	0.5	27.9	0.0113	1.9

* Hy: hydrogenation, Dehy: dehydrogenation.

** C14 cell volume expansion compared to the cell volume of the alloy after ~~fabrication~~synthesis.

*** Heterogeneous strain compared to the heterogeneous strain of the alloy after ~~fabrication~~synthesis.

Formatted Table